European Journal of Medicinal Chemistry 214 (2021) 113190

Contents lists available at ScienceDirect

European Journal of Medicinal Chemistry

journal homepage: http://www.elsevier.com/locate/ejmech

Research paper

Pharmacological characterization of a new series of carbamoylguanidines reveals potent agonism at the H_2R and D_3R

Sabrina Biselli [a, b], Merlin Bresinsky [a], Katharina Tropmann [a], Lisa Forster [a], Claudia Honisch [a, c], Armin Buschauer [a, 1], Günther Bernhardt [a], Steffen Pockes [a, d, e, *]

[a] Institute of Pharmacy, University of Regensburg, Universitätsstraße 31, D-93053, Regensburg, Germany
[b] Agrolab Labor GmbH, 84079, Bruckberg, Germany
[c] Institute of Biomolecular Chemistry – National Research Council (ICB-CNR), Padua Unit Via F. Marzolo, 1, 35131, Padova, Italy
[d] Department of Neurology, University of Minnesota, Minneapolis, MN, 55455, USA
[e] Department of Medicinal Chemistry, Institute for Therapeutics Discovery and Development, University of Minnesota, Minneapolis, MN, 55414, USA

ARTICLE INFO

Article history:
Received 20 November 2020
Received in revised form
31 December 2020
Accepted 8 January 2021
Available online 19 January 2021

Keywords:
Histamine H_2 receptor
Receptor subtype selectivity
Dopamine D_{2long} receptor
Dopamine D_3 receptor
Carbamoylguanidines
Aminothiazoles

ABSTRACT

Even today, the role of the histamine H_2 receptor (H_2R) in the central nervous system (CNS) is widely unknown. In previous research, many dimeric, high-affinity and subtype-selective carbamoylguanidine-type ligands such as UR-NK22 (**5**, $pK_i = 8.07$) were reported as H_2R agonists. However, their applicability to the study of the H_2R in the CNS is compromised by their molecular and pharmacokinetic properties, such as high molecular weight and, consequently, a limited bioavailability. To address the need for more drug-like H_2R agonists with high affinity, we synthesized a series of monomeric (thio)carbamoylguanidine-type ligands containing various spacers and side-chain moieties. This structural simplification resulted in potent (partial) agonists (guinea pig right atrium, [^{35}S]GTPγS and β-arrestin2 recruitment assays) with human (h) H_2R affinities in the one-digit nanomolar range (pK_i (**139**, UR-KAT523): 8.35; pK_i (**157**, UR-MB-69): 8.69). Most of the compounds presented here exhibited an excellent selectivity profile towards the hH_2R, e.g. **157** being at least 3800-fold selective within the histamine receptor family. The structural similarities of our monomeric ligands to pramipexole (**6**), a dopamine receptor agonist, suggested an investigation of the binding behavior at those receptors. The target compounds were (partial) agonists with moderate affinity at the $hD_{2long}R$ and agonists with high affinity at the hD_3R (e.g. pK_i (**139**, UR-KAT523): 7.80; pK_i (**157**, UR-MB-69): 8.06). In summary, we developed a series of novel, more drug-like H_2R and D_3R agonists for the application in recombinant systems in which either the H_2R or the D_3R is solely expressed. Furthermore, our ligands are promising lead compounds in the development of selective H_2R agonists for future in vivo studies or experiments utilizing primary tissue to unravel the role and function of the H_2R in the CNS.

1. Introduction

G protein coupled receptors (GPCRs) constitute one of the most important bioactive complexes in humans and are composed of seven transmembrane domains with three extracellular and three intracellular loops [1,2]. Their versatile role in cell signal transduction makes these proteins valuable pharmacological targets to be exploited by the pharmaceutical industry and in academic research [1,2]. A well-studied GPCR subclass is the histamine receptor family (H_1R, H_2R, H_3R, and H_4R), which belongs to the rhodopsin-like family (class A) [3–6]. Among these, the histamine H_2 receptor (H_2R) [7] has been the subject of many research investigations due to its occurrence in a variety of tissues and cells (e.g. leukocytes, heart, airways, uterus, vascular smooth muscles) and in the brain [3,8,9]. Therefore, numerous H_2R agonists and antagonists have been identified. However, only antagonists have found use in the clinic (e.g. for the treatment of gastroesophageal reflux disease and gastroduodenal ulcer) [3,4]. H_2R agonists, on the

* Corresponding author. Institute of Pharmacy, Faculty of Chemistry and Pharmacy, University of Regensburg, Regensburg, 93053, Germany.
E-mail address: steffen.pockes@ur.de (S. Pockes).
[1] Deceased, July 18, 2017.

https://doi.org/10.1016/j.ejmech.2021.113190
0223-5234/

other hand, have been employed as pharmacological tools in vitro or in vivo to provide further insight into the pharmacological properties of the H_2R, especially to elucidate its role in the central nervous system (CNS).

Within the last decades numerous agonists for the H_2R were developed (Fig. 1). However, most of these ligands cannot be used to study the role of CNS-located H_2Rs in detail due to their respective individual drawbacks. The low potency of the endogenous H_2R ligand histamine (**1,** Fig. 1) could be improved by compounds of the guanidine-type (e.g. arpromidine (**2**), Fig. 1) with significantly higher potency. However, protonation of the strongly basic guanidine group under physiological conditions leads to insufficient oral bioavailability and lack of CNS penetration [10]. During further studies, acylated guanidines with reduced basicity and similar potency were developed [10]. Subsequent bioisosteric replacement of the imidazole ring by an amino(methyl)thiazole moiety, derived from amthamine (**3**, Fig. 1), finally led to the desired selectivity towards the H_2R (cf. **4**, Fig. 1) [11]. The potency of such ligands was further increased by connecting two acylguanidine pharmacophores via an alkyl spacer, resulting in dimeric ligands [12,13]. Recently, dimeric carbamoylguanidine analogues (e.g. UR-NK22 (**5**), Fig. 1) with enhanced stability properties with respect to hydrolytic cleavage, have been reported [14]. However, empirical studies suggest high (oral) bioavailability only for ligands which follow the "rule of five" [15–17]. Despite their high potency and stability, dimeric ligands fail to meet most of those criteria. Moreover, studies with radioactively or fluorescently labeled dimeric carbamoylguanidines indicated a high unspecific binding and receptor independent uptake in cells [14].

The aim of this study was the development of a series of aminothiazole-containing carbamoylguanidine-type ligands with improved and enhanced drug-like properties while possessing the high H_2R subtype selectivity and potency of the dimeric ligands. Therefore, the complexity and size of the compounds was reduced to ligands consisting of a single pharmacophore and a non-polar side chain. There are significant structural similarities between these H_2R ligands and dopamine $D_{2/3}$ receptor ($D_{2/3}R$) agonists (e.g. pramipexole (**6**) [18,19], (−)-19 (**7**) [20], Figure 1). Since dopamine receptors play an important role in the brain, the binding behavior of our ligands at these receptors was investigated in order to avoid experimental bias. Herein we report the synthesis, as well as the chemical and pharmacological characterization (competition binding-, [^{35}S]GTPγS-, β-arrestin2 recruitment- and guinea pig (gp) right atrium assays) of novel, monomeric carbamoylguanidine-type H_2R ligands and the first investigations (competition binding- and β-arrestin2 recruitment assays) of such ligands at the dopamine D_{2long} and D_3 receptors.

2. Results and discussion

2.1. Chemistry

The preparation of the monomeric N^G-carbamoylated guanidines **138**–**172** and **179**–**186** was performed by guanidinylation of the amine building blocks **9a/b** or **11**–**12** in analogy with the isocyanate-based procedure developed for the dimeric N^G-carbamoylated guanidines (Scheme 1) [14]. The (thio)carbamoylguanidines **173**–**178** were prepared using the guanidine building block **10** and a slightly modified procedure (Scheme 1), due to the less reactive isothiocyanates, in comparison to isocyanates [21]. The required building blocks mono-Boc-protected *S*-methylisothiourea **8**, the amines **9a/b** and **11**–**12**, and the guanidine **10** were synthesized as previously published or as described in the Supplementary Material (SM) (cf. Scheme 1, S1 and S2, SM) [11].

The Boc-protected isothioureas **48**–**82** play a central role as guanidinylating reagents in the synthesis of the target compounds. They were synthesized by treatment of **8** with the respective isocyanates in the presence of triethylamine (TEA) or Hünig's base (DIPEA). The isocyanates were either commercially available (**34**–**39**) or prepared by two different strategies starting from the corresponding amines **13**–**33** using triphosgene/phosgene or from the branched carboxylic acids **40**–**47** applying the Curtius rearrangement. The respective amines **13**–**16**, **18**, **20**–**23**, **28** and **31**–**33** were commercially available while **17**, **19**, **24**–**27** and **29**–**30** were synthesized from commercially available ketones (cf. Scheme S3, SM). The respective carboxylic acids were synthesized as previously described [11]. Because of their instability the intermediate isocyanates were not isolated, but immediately reacted with **8** in a one-pot reaction. The protected N^G-carbamoylated guanidines **89**–**123** and **130**–**137** were prepared by treating the amine building blocks **9a/b** or **11**–**12** with the respective Boc-protected isothioureas (**48**–**82**) in the presence of $HgCl_2$ and TEA. The synthesis of the Boc-protected (thio)carbamoylguanidines **124**–**129** started with the conversion of amines **14**–**16** and **31**–**33** with

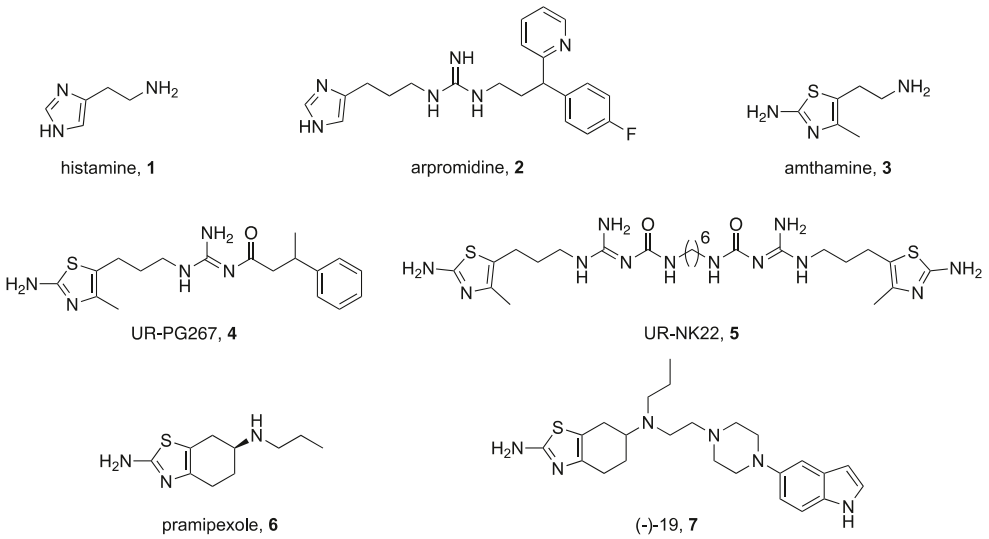

Fig. 1. Structures of histamine (**1**), representative monomeric and dimeric H_2R agonists (**2**–**5**), and the $D_{2/3}R$ agonists pramipexole (**6**) and (−)-19 (**7**).

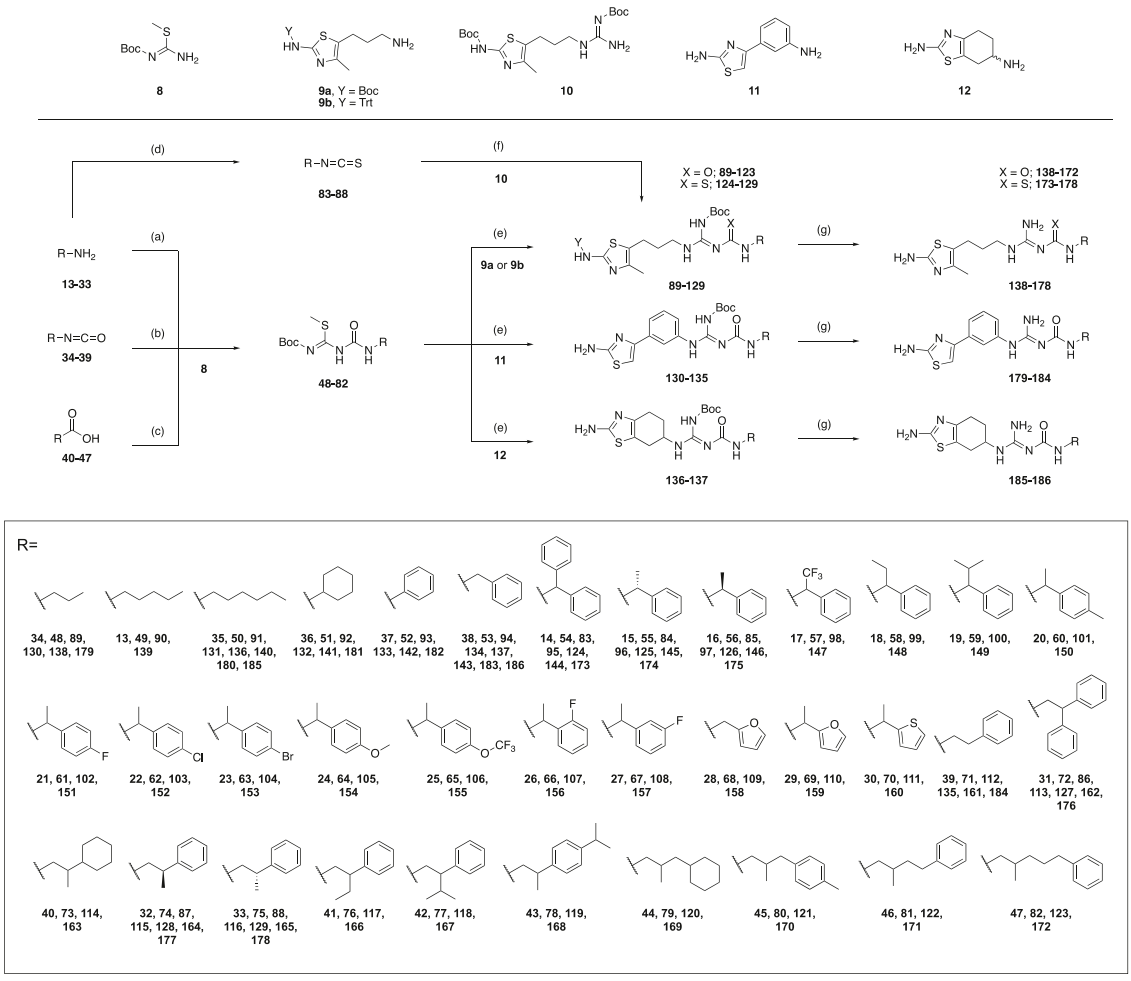

Scheme 1. Synthesis of the monomeric (thio)carbamoylguanidine-type ligands **138**–**186**. Reagents and conditions: (a) 15% phosgene in toluene or triphosgene, DIPEA, DCM, (Ar-atmosphere), 5–30 min, 0 °C → **8**, 2–3 h, room temperature (rt); (b) **8**, TEA, DCM, overnight, rt; (c) oxalyl chloride, DMF (cat.), DCM, Ar-atmosphere, 0 °C-rt, 25 min → NaN_3, acetone/H_2O, 30 min, 0 °C → DCM, reflux, 30 min → **8**, TEA, DCM, rt, overnight; (d) thiophosgene, $NaHCO_3$, DCM/H_2O, rt, 30 min; (e) $HgCl_2$, TEA, DCM, (Ar-atmosphere), rt, overnight; (f) DCM, reflux, 3–4 days; (g) TFA, DCM, rt or reflux, overnight.

thiophosgene to the corresponding isothiocyanates **83**–**88**. In the next step, these isothiocyanates were converted with the guanidine building block **10** under reflux (dichloromethane (DCM)) to give the respective Boc-protected N^G-(thio)carbamoylated intermediates **124**–**129**. Finally, the resulting precursors **89**–**137** were treated with trifluoroacetic acid (TFA) to obtain the title compounds **138**–**186** with high purity (cf. Figs. S24–S72, SM) after purification with preparative HPLC or recrystallization with HCl/1,4-dioxane/diethyl ether.

The chemical stability of the representative carbamoylguanidines **141**, **142** and **161** and related acylguanidines is shown in the SM (Figs. S73–S79).

2.2. Determination of pK_a values and in silico ADME

In vivo behavior, including bioavailability and CNS permeability, of a compound is influenced by its physicochemical properties [15,22]. In addition, information about the substance-specific acid-base properties are of great importance. Empirical studies by others have revealed a marked cut off for CNS distribution of bases, since no known CNS-penetrable compound has a pK_a over 10.5 [22]. As already explained in the introduction, acylguanidines represent a class of compounds with improved physicochemical properties ($pK_a \approx 8$) compared to the strongly basic guanidine-type ligands ($pK_a \approx 12$–13) [10]. It is widely assumed, that the more chemically stable carbamoylguanidines have a similar basicity to their acylguanidine counterparts, but there is no experimental data available to support that assumption. Therefore, we determined the pK_a values of **145** (UR-Po563) containing both a carbamoylguanidine and an aminothiazole motif, as well as **213** and **216** (for synthesis see SM, Scheme S4) incorporating solely the carbamoylguanidine motif and the aminothiazoles **217** and **218** (Table 1a).

The pK_a values were determined by titration of the free base (**145**) with 1 M HCl or the titration of the HCl salts (**213** and **216**–**218**) with 0.01 or 0.1 M NaOH in aqueous solution or ethanol (EtOH). These titrations were performed in the presence of a freshly calibrated glass electrode and the pK_a values were determined from the half-equivalence point (cf. Figs. S82–S86, SM). Compounds **213** and **216**–**218** were used as HCl salts due to their superior solubility in water and EtOH compared to the corresponding TFA salts. Apart from the commercially available HCl salts of **217** and **218**, TFA salts of compounds **213** and **216** were prepared as hydrochlorides using 5–6 N HCl in 2-propanol and diethyl ether, as described in the SM (cf. **213** and **216**). The pK_a values were in good agreement with both the published data and calculated values (Table 1a). These results confirm that the carbamoylguanidine motif possesses a similar pK_a compared to the acylguanidine motif.

In addition to the determination of pK_a values an in silico study

Table 1a
Comparison of the determined pK_a values with reference data.

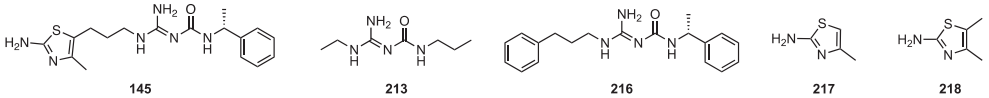

Cmpd.	pK_a[a]	reference/predicted pK_a
145	4.68 ± 0.02 (pK_{a1}) 7.47 ± 0.04 (pK_{a2})	–
213	8.31 ± 0.02	–
216	7.96 ± 0.01	–
217	5.77 ± 0.02	5.95[b]; 4.64[c]; 5.36 ± 0.10[e]
218	6.28 ± 0.04	6.29[d]; 5.97 ± 0.10[e]

[a]pK_a values were determined by manual titration of the free base (**145**) with 1 M HCl or HCl salts (**213** and **216**–**218**) with 0.01 or 0.1 M NaOH at rt. Data shown are means ± SEM of 3 independent experiments. [b]The exact titration conditions were not reported in the literature. The authors only stated, that an aqueous solution was titrated [23,24]. [c]pK_a value was determined by titration of an aqueous solution of the free base with 0.5 M HCl at rt using a pH meter [25]. [d]pK_a value was determined by a spectrometric method in aqueous solution containing 4% EtOH at 26 °C [24,26]. [e]Predicted pK_a values from SciFinder (conditions: most basic, T = 25 °C).

predicting several crucial physicochemical and pharmacokinetic parameters of representative monomeric (**139**, **157** and **163**) and dimeric carbamoylguanidines (UR-NK22 (**5**) [14], UR-NK41 (**219**) [14] and UR-NK53 (**220**) [14]) was conducted. Moreover, compounds which are reported to be orally bioavailable and CNS penetrable such as the anti-Parkinson agent pramipexole (**6**) and the acylguanidines UR-AK24 (**221**) [10] and UR-PG126 (**222**) [10] were included for comparison. To obtain the data, the SwissADME web tool [27] was employed and the results are summarized in Table 1b. As expected, the monomeric ligands (**139**, **157** and **163**) match Lipinski's rule of five [15] and Ghosen's extension [16], while the dimeric ligands suffer from several violations, e.g. due to their molecular size. In addition, the monomeric ligands possess more favorable properties including lower topological polar surface area (TPSA) (monomeric: 146.66 Å^2 vs. dimeric: 293.32 Å^2, Table 1b) and higher bioavailability (Abbot bioavailability score [28]; monomeric: 0.55 vs. dimeric: 0.17, Table 1b) if compared with their dimeric counterparts. On the other hand, we were surprised that all compounds including **6** and **221**–**222** were predicted to be "not blood brain barrier (BBB) permeant" although experimental evidence suggests the contrary [10]. We believe that these predicted results might indicate a potential limit of this in silico model since ionic

Table 1b
In silico determined physicochemical and pharmacokinetic properties (ADME).

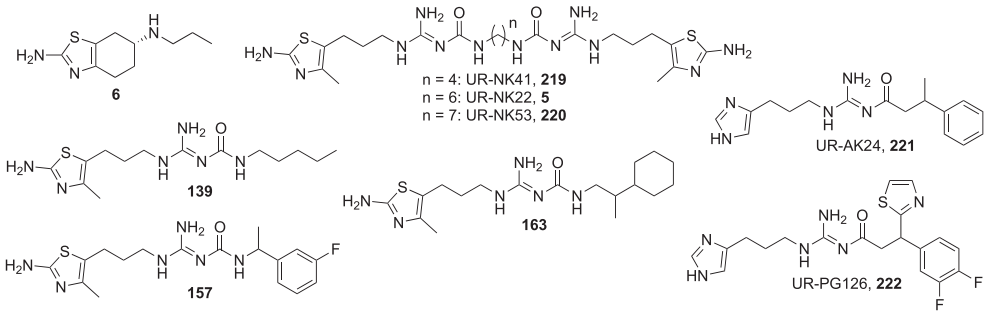

Properties	139	157	163	219	5	220	221	222	6
MW/g/mol	326.5	378.5	380.6	566.8	594.8	608.8	313.4	418.6	211.3
Rotatable bonds	11	9	10	19	21	22	9	10	3
HBA	3	4	3	6	6	6	3	6	2
HBD	4	4	4	8	8	8	3	3	2
Molar refractivity	92.3	102.3	109.4	153.6	163.3	168.1	91.1	106.4	61.2
TPSA/Å^{2a}	146.7	146.7	146.7	293.3	293.3	293.3	96.2	137.3	79.2
Lipophilicity, logP^b	2.10	2.54	3.03	1.70	2.28	2.55	2.09	3.08	1.88
Solubility, logS^c	−2.96	−3.69	−4.43	−3.66	−4.15	−4.50	−2.99	−3.87	−2.39
% human oral absorption^d	58	58	58	8	8	8	76	62	82
BBB permeant	No	No	No	No	No	No	No	No	No
Bioavailability^e	0.55	0.55	0.55	0.17	0.17	0.17	0.55	0.55	0.55
Druglikeness^f	Yes	Yes	Yes	No	No	No	Yes	Yes	Yes

[a]TPSA: topological polar surface area: this parameter correlates with human intestinal absorption (empirical data suggest a value < 140) [30]. [b]Consensus logP [27]: average of five predictions (iLOGP [31], XLOGP3 [32], WLOGP [33], MLOGP [34,35] and SILICOS-IT [27]). [c]LogS values were calculated with ESOL [36]: insoluble < −10 < poorly < −6 < moderately < −4 < soluble < −2 < very < 0 < highly. [d]The percentage of human oral absorption was calculated using the TPSA by the formula, % human oral absorption = 109 − (0.345 x TPSA), > 89%: high, < 25%: poor [37]. [e]Abbot bioavailability score; 0.55: 55% of the neutral, zwitterionic, or cationic compounds that pass the Lipinski criteria have >10% bioavailability; 0.17: 17% of those that fail have > 10% bioavailability [28]. [f]Lipinski criteria [15] (molecular weight (MW) ≤ 500, H-bond donors (HBD) ≤ 5, H-bond acceptors (HBA) ≤ 10, logP ≤ 5); Ghose criteria [16] (160 ≤ MW ≤ 480, −0.4 ≤ logP ≤ 5.6, 40 ≤ molar refractivity ≤ 130, 20 ≤ atom number ≤ 70). The bioavailability radars generated with SwissADME web tool [27] are shown in Fig. S96 in the SM.

transport which is postulated for pramipexole (**6**) [29], can probably not be calculated.

Since the compounds **139**, **157** and **163**, containing both an aminothiazole and a carbamoylguanidine partial structure, possess appropriate pK_a values as well as good physicochemical and pharmacokinetic properties, we believe that our optimization and simplification strategy was in many cases very successful. The obtained in silico data indicate that the compounds **139**, **157** and **163** are more drug-like than their dimeric counterparts and should be promising lead structures for the elucidation of the role of the H_2R in the CNS.

2.3. Pharmacology

2.3.1. Binding affinities at the human histamine receptor family

The (thio)carbamoylated guanidines **138**–**186** were investigated in radioligand competition binding experiments to elucidate their structure-affinity relationships at the hH_2R and their selectivity over the hH_1R, hH_3R and hH_4R subtypes. The results are presented in Table 2 as binding constants (pK_i values), determined on membrane preparations of Sf9 insect cells expressing the $hH_{1\text{-}4}R$, respectively. Radioligand displacement curves of representative compounds are shown in Fig. 2 and additional curves are shown in the SM (Figs. S87–S89). In case of the aminothiazolylpropyl carbamoylguanidines, a large number of variations of the residue R were well tolerated, leading to high affinity hH_2R ligands with pK_i values over 7 (compounds: **138**–**172**). However, there were some exceptions: e.g. a cyclohexyl (**141**) or a phenyl (**142**) residue resulted in low to moderate hH_2R affinity with pK_i values of 5.50 and 6.77 (Table 2). This leads to the assumption that bulky substituents are not well tolerated in very close proximity to the carbamoylguanidine function. The hH_2R affinity of aminomethylthiazolylpropyl carbamoylated guanidines with a terminal n-alkyl residue was dependent on the chain length (**138**–**140**). While the n-propyl containing ligand **138** showed a moderate affinity with a pK_i value of 6.98, the ligands containing a n-hexyl or n-pentyl residue showed higher affinities with pK_i values of 7.54 (**140**) and 8.35 (**139**, UR-KAT523) (Table 2). Interestingly, most of the ligands investigated containing a benzyl residue with or without further substituents (**143**–**157**) showed high hH_2R affinities with pK_i values over 7. Only the trifluoromethyl containing ligands **147** and **155** showed moderate affinities with pK_i values of 6.64 and 6.90 (Table 2). Branched residues were also well-tolerated as were the introduction of a phenyl, methyl, ethyl or isopropyl substituents (ligands **144**–**149**: pK_i: 7.2–7.8) which resulted in no change or even an increase of affinity compared to the unbranched analogue (pK_i (**143**): 7.16) (Table 2). Furthermore, substituents in ortho-, meta- and para-position of the phenyl ring of the branched 1-phenyleth-1-yl containing ligands were also well tolerated. Methyl, fluoro-, chloro-, bromo- and methoxy-substituents in the para or a fluoro-substituent in the ortho position led to high affinity hH_2R ligands with pK_i values of 7.3–7.5 (ligands **150**–**154** and **156**) (Table 2). Noteworthily, a fluoro-substituent in the meta position of the phenyl ring of the 1-phenyleth-1-yl residue (**157**, UR-MB-69) resulted in an increased affinity (pK_i: 8.69) compared to the para or ortho fluoro-substituted ligands (pK_i (**151**): 7.50 and pK_i (**156**): 7.54) (Table 2). Heteroarene (e.g. fur-2-yl-methyl, 1-(fur-2-yl)-eth-1-yl or 1-(thiophen-2-yl)-eth-1-yl) containing ligands (**158**–**160**) showed high hH_2R affinities with pK_i values of 7.2–8.0 (Table 2). A 2-phenyl-eth-1-yl scaffold as a residue resulted in aminothiazolylpropyl carbamoyl guanidines (**161**, **162** and **164**–**168**) with pK_i values of around 7. The introduction of an aliphatic 2-cyclohexyl-eth-1-yl residue (**163**) resulted in a slightly higher affinity with a pK_i value of 7.40 compared to the aromatic counterpart (pK_i (**164**): 7.16) (Table 2). Aminothiazolylpropyl carbamoylated guanidines with residues containing longer linkers, as represented in **169**–**172**, showed high affinities with pK_i values of 7.1–7.2 (Table 2), but did not bring a significant improvement in ligand affinity at the hH_2R. All attempted modifications of the aminothiazolylpropyl carbamoylguanidine pharmacophore (**173**–**186**), for example, by rigidization of the aminothiazolylpropyl moiety or the bioisosteric replacement of the carbamoylguanidine by a thiocarbamoylguanidine, resulted in low to moderate hH_2R affinity ligands with pK_i values of 3.4–6.9 (Table 2). All investigated ligands showed a low affinity at the other hHR subtypes ($hH_{1,3,4}Rs$) with pK_i values of 4.1–5.9 (Table 2). The high affinity at the hH_2R combined with the low affinity at the other subtypes led to an excellent subtype selectivity (3–4 orders of magnitude) for the ligands **139** and **157**–**159**. The ligands **139**, **157** and **158** showed similar or even higher hH_2R affinities (pK_i values of 8.35, 8.69 and 7.98) than the already described dimeric aminothiazole containing carbamoylguanidine UR-NK22 (**5**) [14] (pK_i: 8.07 [14]) (Table 2). In addition, the subtype selectivity of these small molecules (molecular weight: < 400 g/mol) is improved compared to the bulky dimeric ligands like **5** and analogues (molecular weight: > 550 g/mol). A summary of the structure-affinity relationships based on the H_2R affinity of the synthesized carbamoylguanidines is presented in Fig. 3.

The influence of the stereochemistry on hH_2R affinity and subtype selectivity was investigated based on the enantiomeric pairs **145** and **146**, **164** and **165**, **174** and **175**, as well as **177** and **178**. The enantiomeric pairs showed only slight differences in hH_2R affinity and subtype selectivity. For example, the ligands **145** (pK_i: 7.75) and **174** (pK_i: 6.94) with (R)-configuration tended to show slightly higher hH_2R affinities when compared to their counterparts **146** (pK_i: 7.29) and **175** (pK_i: 6.47) with (S)-configuration (Table 2). The enantiomeric purity of **145**, **146**, **164**, **165**, **174**, **175**, **177** and **178** was determined as described in the SM (Figs. S80–S81).

2.3.2. Functional characterization of selected (thio) carbamoylguanidines at the guinea pig/human H_2Rs

The aminothiazoles **138**–**186** were investigated for gp/hH_2R agonism in the guinea pig right atrium assay [39,41] (gpH_2R) (Table 3 and Fig. S90, SM), the [^{35}S]GTPγS binding assay [14,39,42,43] (hH_2R) and/or the β-arrestin2 recruitment assay [43–45] (hH_2R) (Table 4). The aminothiazolylpropyl containing N^G-carbamoylated guanidines **139**, **140**, **144**–**154**, **156**–**160**, **164** and **165** showed high agonistic activities at the gpH_2R with pEC_{50} values of 7.3–8.2 and were primarily strong partial or even full agonists (e.g. **146**, **149** and **159**) (Table 3). Only the carbamoylguanidines **155** and **162** were moderately active partial agonists with pEC_{50} values of 6.14 and 6.76 (Table 3). The N^G-thiocarbamoylated guanidines **173**–**178** were partial agonists at the gpH_2R with pEC_{50} values of 6.3–7.2 (Table 3). The bulky ligand **176** was inactive at the gpH_2R within the concentration range of the assay. The highest potencies at the gpH_2R were shown by the n-pentyl residue-containing ligand **139** (pEC_{50}: 8.24) and the 2-phenyl-eth-2-yl residue-containing ligand **145** with (R)-configuration (pEC_{50} value of 8.12): both appearing as strong partial agonists (α: 0.78 and 0.95, respectively) (Table 3). The high affinity hH_2R ligand **157** (pK_i: 8.69) was a strong partial agonist (α: 0.85) at the gpH_2R with a pEC_{50} value of 7.58 (Table 3). The enantiomeric pairs **145** and **146**, **164** and **165**, **174** and **175**, as well as **177** and **178** showed only slight differences in agonistic potency and efficacy with eudismic ratios (EC_{50} value of the eutomer divided by EC_{50} value of the distomer) ranging from 2.0 to 3.3. The ligands **145** (pEC_{50}: 8.12) and **174** (pEC_{50}: 7.05) with (R)-configuration tended to possess higher gpH_2R potencies when compared to their counterparts **146** (pEC_{50}: 7.63) and **175** (pEC_{50}: 6.65) with (S)-configuration (Table 3). On the

Table 2
Affinities of the monomeric (thio)carbamoylated guanidines **138**–**186** at the $hH_{1-4}R$, obtained from competition binding studies on membrane preparations of Sf9 insect cells expressing the respective histamine receptor subtype.

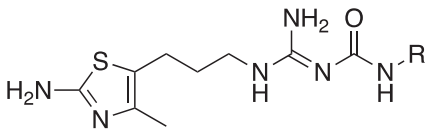

138-172

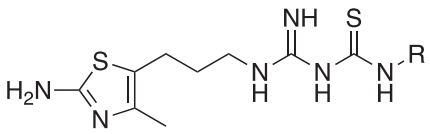

173-178

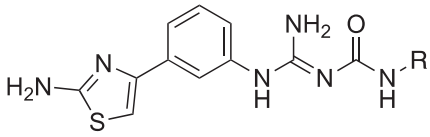

179-184

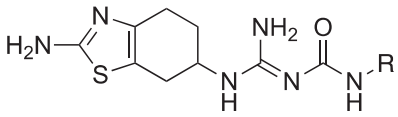

185-186

Cmpd.	R	pK$_i$								Selectivity ratios of K_i
		hH_1R[a]	N	hH_2R[b]	N	hH_3R[c]	N	hH_4R[e]	N	(H_1R/H_2R/H_3R/H_4R)
1	–	5.62 ± 0.03 [39]	3	6.58 ± 0.04 [39]	48	7.59 ± 0.01 [39]	42	7.60 ± 0.01 [39]	45	9/1/0.1/0.1
5	–	6.06 ± 0.05 [14]	2	8.07 ± 0.05 [14]	3	5.94 ± 0.16 [14]	3	5.69 ± 0.07 [14]	4	102/1/135/240
6	–	n.d.	–	4.86 ± 0.07	5	n.d.	–	n.d.	–	–
138		4.54 ± 0.02	3	6.98 ± 0.11	3	4.35 ± 0.01	3	4.06 ± 0.06	2	275/1/427/832
139		4.97 ± 0.10	3	8.35 ± 0.08	3	4.98 ± 0.17	3	5.37 ± 0.09	3	2399/1/2344/955
140		5.11 ± 0.03	3	7.54 ± 0.07	4	5.25 ± 0.02	3	5.09 ± 0.02	2	269/1/195/282
141		4.61 ± 0.09	3	6.77 ± 0.27	3	n.d.	–	4.50 ± 0.06	2	145/1/-/186
142		n.d.	–	5.50 ± 0.08	3	n.d.	–	4.65 ± 0.05	2	-/1/-/7
143		5.21 ± 0.02	3	7.16 ± 0.05	3	4.71 ± 0.05	3	4.72 ± 0.09	2	89/1/282/275
144		4.80 ± 0.02	3	7.36 ± 0.01	3	5.04 ± 0.08	3	5.20 ± 0.04	3	363/1/209/145
145		5.06 ± 0.05	3	7.75 ± 0.05	3	4.36 ± 0.04	3	4.87 ± 0.01	3	490/1/2455/759
146		4.67 ± 0.06	3	7.29 ± 0.04	3	4.48 ± 0.02	3	4.75 ± 0.01	3	417/1/646/347
147		4.27 ± 0.02	3	6.64 ± 0.02	3	4.50 ± 0.02	3	4.76 ± 0.08	3	234/1/138/76
148		4.90 ± 0.04	3	7.20 ± 0.04	3	4.66 ± 0.02	3	4.95 ± 0.03	3	200/1/347/178
149		4.61 ± 0.14	3	7.45 ± 0.02	3	4.72 ± 0.05	3	5.10 ± 0.10	3	692/1/537/224
150		5.29 ± 0.04	3	7.51 ± 0.04	3	4.58 ± 0.03	3	4.95 ± 0.01	3	166/1/851/363
151		4.99 ± 0.03	3	7.50 ± 0.06	3	4.59 ± 0.04	3	4.86 ± 0.04	3	324/1/813/437
152		5.35 ± 0.04	3	7.33 ± 0.03	3	4.75 ± 0.02	3	5.07 ± 0.01	3	95/1/380/182
153		5.54 ± 0.01	3	7.52 ± 0.06	3	4.89 ± 0.01	3	5.09 ± 0.03	3	95/1/427/269

Table 2 (*continued*)

Cmpd.	R	pK_i								Selectivity ratios of K_i
		hH_1R[a]	N	hH_2R[b]	N	hH_3R[c]	N	hH_4R[e]	N	(H_1R/H_2R/H_3R/H_4R)
154		5.23 ± 0.06	3	7.43 ± 0.03	3	4.48 ± 0.04	3	4.70 ± 0.03	3	158/1/891/537
155	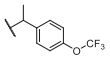	4.66 ± 0.13	3	6.90 ± 0.07	3	4.84 ± 0.07	3	5.09 ± 0.07	3	174/1/115/65
156		4.77 ± 0.10	3	7.54 ± 0.02	3	4.51 ± 0.06	3	4.89 ± 0.03	3	589/1/1072/447
157		5.11 ± 0.10	3	8.69 ± 0.10	3	4.41 ± 0.06	3	4.88 ± 0.01	3	3802/1/19055/6457
158		4.62 ± 0.09	3	7.98 ± 0.01	3	4.13 ± 0.01	3	4.12 ± 0.06	3	2291/1/7079/7244
159		4.34 ± 0.11	3	7.50 ± 0.08	3	4.36 ± 0.07	3	4.34 ± 0.05	3	1445/1/1380/1445
160		4.59 ± 0.02	3	7.20 ± 0.03	3	4.23 ± 0.01	3	4.52 ± 0.03	3	407/1/933/479
161		n.d.	–	6.80 ± 0.20	4	n.d.	–	4.83 ± 0.06	2	-/1/-/93
162		5.28 ± 0.01	3	7.06 ± 0.04	3	5.00 ± 0.01	3	5.31 ± 0.03	3	60/1/115/56
163		5.63 ± 0.06	3	7.40 ± 0.01	2	5.00 ± 0.08	3	5.72 ± 0.05[f]	3	59/1/251/48
164		5.06 ± 0.06	3	7.00 ± 0.05	3	4.77 ± 0.05	3	4.92 ± 0.02	3	87/1/170/120
165		5.02 ± 0.05	3	6.99 ± 0.06	3	4.57 ± 0.06	3	4.87 ± 0.01	3	93/1/263/132
166		5.10 ± 0.08	3	7.11 ± 0.03	3	4.78 ± 0.03[d]	3	5.17 ± 0.02[f]	3	102/1/214/87
167		5.23 ± 0.03	3	6.99 ± 0.05	3	4.93 ± 0.03[d]	3	5.23 ± 0.03[f]	3	58/1/115/58
168	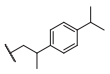	5.31 ± 0.02	3	6.83 ± 0.08	3	5.10 ± 0.02[d]	3	5.58 ± 0.01	3	33/1/54/18
169		5.42 ± 0.07	3	7.15 ± 0.02	4	5.13 ± 0.01[d]	3	5.43 ± 0.01[f]	3	54/1/105/52
170	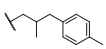	5.78 ± 0.13	3	7.14 ± 0.08	2	5.49 ± 0.01	3	5.44 ± 0.02	3	23/1/45/50
171	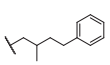	5.87 ± 0.09	3	7.20 ± 0.04	3	5.04 ± 0.04[d]	3	5.49 ± 0.08[f]	3	21/1/145/51
172	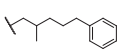	5.15 ± 0.07	3	7.22 ± 0.05	3	5.64 ± 0.08	3	6.11 ± 0.13	3	117/1/38/13
173		4.33 ± 0.01	3	6.22 ± 0.10	3	4.36 ± 0.06	3	4.63 ± 0.02	3	78/1/72/39
174		3.96 ± 0.07	3	6.94 ± 0.08	3	4.19 ± 0.03	3	4.57 ± 0.01	3	955/1/562/234
175		4.11 ± 0.06	3	6.47 ± 0.05	3	4.09 ± 0.07	3	4.26 ± 0.02	3	229/1/240/162

(*continued on next page*)

Table 2 (*continued*)

Cmpd.	R	pK$_i$								Selectivity ratios of K_i
		hH$_1$R[a]	N	hH$_2$R[b]	N	hH$_3$R[c]	N	hH$_4$R[e]	N	(H$_1$R/H$_2$R/H$_3$R/H$_4$R)
176		4.35 ± 0.01	3	5.84 ± 0.02	3	4.33 ± 0.06	3	4.67 ± 0.02	3	31/1/32/15
177		4.20 ± 0.03	3	5.94 ± 0.06	3	4.16 ± 0.03	3	4.35 ± 0.01	3	55/1/60/39
178		4.28 ± 0.01	3	6.37 ± 0.06	3	4.08 ± 0.10	3	4.49 ± 0.02	3	123/1/195/76
179		n.d.	–	5.28 ± 0.06	4	n.d.	–	<4.0	2	-/1/-/>19
180		n.d.	–	6.16 ± 0.07	4	4.96 ± 0.07	3	5.02 ± 0.06	2	-/1/16/14
181		n.d.	–	5.35 ± 0.02	3	n.d.	–	4.87 ± 0.03	2	-/1/-/3
182		n.d.	–	3.43 ± 0.07	3	n.d.	–	4.19 ± 0.10	2	-/1/-/0.2
183		n.d.	–	5.70 ± 0.10	3	n.d.	–	4.46 ± 0.01	2	-/1/-/17
184		n.d.	–	5.40 ± 0.05	3	n.d.	–	4.52 ± 0.13	2	-/1/-/8
185		5.71 ± 0.02	3	5.95 ± 0.06	4	5.82 ± 0.03	3	4.78 ± 0.05	2	2/1/1/15
186		5.92 ± 0.02	3	6.29 ± 0.08	3	5.48 ± 0.06	3	4.52 ± 0.01	2	2/1/6/59

Competition binding assay on membrane preparations of Sf9 insect cells: [a]Co-expression of the hH$_1$R and RGS4 proteins (radioligand: [^{3}H]mepyramine, c = 5 nM, K_d = 4.5 nM). [b]Expression of the hH$_2$R-G$_{s\alpha S}$ fusion protein (radioligand: [^{3}H]UR-DE257 [38], c = 20 nM, K_d = 12.2 nM). [c]Co-expression of the hH$_3$R, G$_{\alpha i2}$, and G$_{\beta 1\gamma 2}$ proteins (radioligand: [^{3}H]UR-PI294 [40] c = 2 nM, K_d = 1.1 nM or. [d][^{3}H]histamine c = 15 nM, K_d = 12.1 nM), or. [e]Co-expression of the hH$_4$R, G$_{\alpha i2}$, and G$_{\beta 1\gamma 2}$ proteins (radioligand: [^{3}H]histamine c = 10 nM, K_d = 15.9 nM or. [f][^{3}H]UR-PI294 [40] c = 5 nM, K_d = 5.1 nM). Data were analyzed by nonlinear regression and were best-fitted to four-parameter sigmoidal concentration-response curves. Data shown are means ± SEM of N independent experiments, each performed in triplicate. n.d.: not determined.

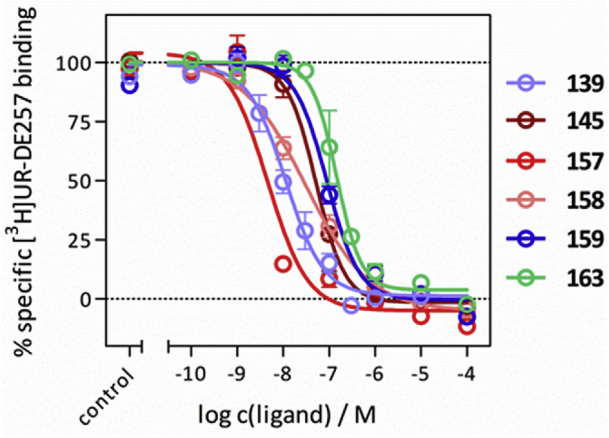

Fig. 2. Displacement of the radioligand [^{3}H]UR-DE257 [38] (c = 20 nM, K_d = 12.2 nM) by increasing concentrations of the respective ligand determined on membrane preparations of Sf9 insect cells expressing the hH$_2$R-G$_{s\alpha S}$ fusion protein. Data represent mean values ± SEM of 2–3 independent experiments, each performed in triplicate.

other hand, the ligands **165** (pEC$_{50}$: 7.89) and **178** (pEC$_{50}$: 6.83) with (S)-configuration tended to possess higher gpH$_2$R potencies compared to their counterparts **164** (pEC$_{50}$: 7.59) and **177** (pEC$_{50}$: 6.31) with (R)-configuration (Table 3). Noteworthy, due to the side chain elongation in **164** and **177** (one methylene group), the orientation of the methyl group in the binding pocket should be identical for all the four eutomers described.

The N^G-carbamoylated guanidines **138**, **140**–**143**, **161**, **163**, **166**–**171** and **185**–**186** were investigated for hH$_2$R agonism in the [^{35}S]GTPγS binding assay on membrane preparations of Sf9 insect cells expressing the hH$_2$R-G$_{s\alpha S}$ fusion protein (Table 4). Compounds **179**–**184** were tested in the antagonistic mode versus histamine to determine their pK_b values. The ligands **138**–**143**, **145**–**146**, **157**, **159**, **161**, **163**, **166**–**172**, **174** and **186** were also investigated for agonism in the β-arrestin2 recruitment assay on HEK293T-β-Arr2-hH$_2$R cells, stably expressing the hH$_2$R-ElucC and βArr2-ElucN fusion constructs [44]. Functional testing in the gpH$_2$R right atrium and β-arrestin2 recruitment assays ensured a comprehensive characterization, at least for the most interesting compounds. The monomeric N^G-carbamoylated amino(methyl)thiazolylpropylguanidines **138**, **140**–**143**, **161**, **163** and **166**–**171** were partial to full agonists in the [^{35}S]GTPγS binding assay and showed moderate to high hH$_2$R potencies with pEC$_{50}$ values of 6.3–7.8 (Table 4). The benzyl residue containing ligand **143** showed a high potency with a pEC$_{50}$ value of 7.54 combined with strong partial agonism. Ligands containing a n-hexyl residue (**140**), a branched 2-phenyl-eth-1-yl residue (**166**–**168**, **170**, and **171**), or a branched 2-cyclohexyl-eth-1-yl residue (**163** and **169**) were highly potent partial agonists with pEC$_{50}$ values of 7.2–7.8 (Table 4). Interestingly, the aminothiazolylphenyl containing ligands **179**–**184** appeared as weak antagonists at the hH$_2$R with pK_b values (4.8–6.1, Table 4) which were in good agreement with the pK_i values obtained (3.4–6.2, Table 2). Introduction of the less flexible 2-amino-4,5,6,7-tetrahydrobenzothiazol-6-yl moiety (**185** and **186**) resulted in partial agonism (**186**, α: 0.57, pEC$_{50}$: 6.67) or weak partial agonism (**185**, α: 0.16, pEC$_{50}$: 5.57) (Table 4). The structurally related dopamine receptor agonist pramipexole (**6**) was also a partial agonist at the hH$_2$R (α: 0.66, pEC$_{50}$: 5.07) (Table 4).

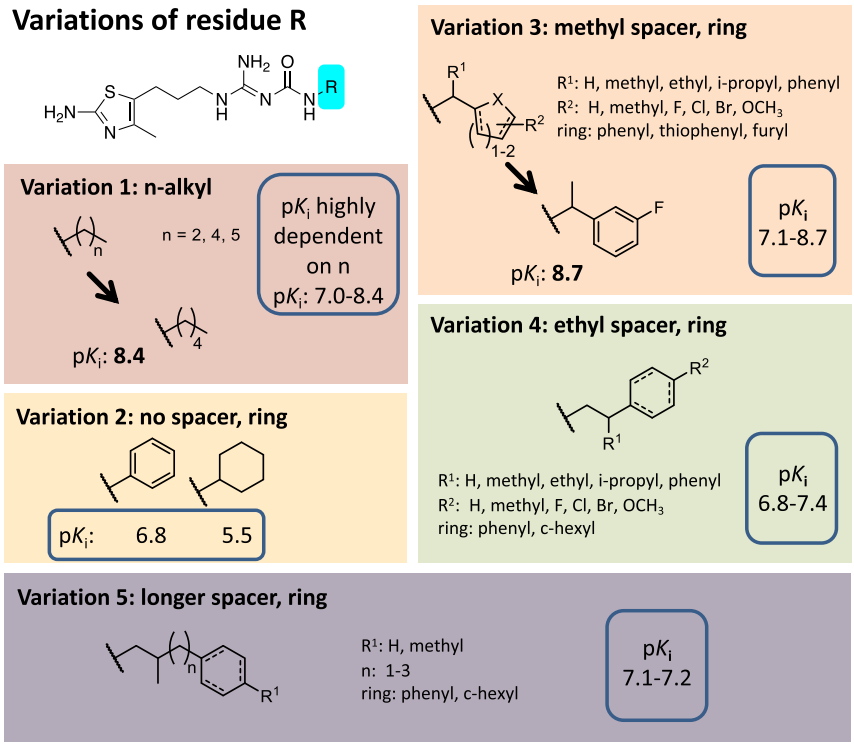

Fig. 3. H_2R affinity of agonistic carbamoylguanidines: summary of structure-affinity relationships.

Ligand characterization in the β-arrestin2 recruitment assay showed that compounds **138**–**143**, **145**–**146**, **157**, **159**, **161**, **163**, **166**–**172**, **174** and **186** were partial agonists with pEC_{50} values of 5.4–7.3 (c.f. Fig. S91, SM). The data obtained were comparable with the [^{35}S]GTPγS assay data but generally lower potencies and efficacies in the β-arrestin2 recruitment assay were observed. The enantiopure ligand **145** and the 1-(3-fluoro-phenyl)eth-1-yl residue containing ligand **156** showed the highest agonistic potencies resulting in pEC_{50} values in the two-digit nanomolar range (7.34 and 7.19) (Table 4). Overall, the (partial) agonists investigated in both [^{35}S]GTPγS and β-arrestin2 recruitment assay showed varying degrees of bias for G protein activation (Fig. S92, SM). This is in agreement with the findings for acylguanidines and dimeric carbamoylguanidines [44].

2.3.3. *Binding affinities at the human $D_{2long}R$ and D_3R*

Aminothiazole containing ligands such as pramipexole (**6**) and its derivatives (e.g. **7**) are described as high affinity dopamine receptor ligands (preferring the D_2-like family) [53]. Because of the structural similarity between pramipexole (**6**) and the N^G-(thio) carbamoylated guanidines that were prepared, selected ligands **139**, **140**, **143**, **145**, **146**, **157**, **159**, **163**, **166**, **169**–**172**, **174**, **180**, **185** and **186** were investigated in competition binding experiments on homogenates of HEK293T-CRE-Luc-hD_{2long}R and HEK293T-CRE-Luc-hD_3R cells using [^{3}H]*N*-methylspiperone as radioligand [54]. The results are summarized in Table 5 and radioligand displacement curves (hD_3R) of representative compounds are shown in Fig. 4.

For the standard agonist pramipexole biphasic displacement curves were reported at the hD_{2long}R with pK_i values for high (p$K_{i/high}$ value) and low (p$K_{i/low}$ value) affinity binding sites [54]. The N^G-(thio)carbamoylated guanidines **139**, **140**, **143**, **145**, **146**, **157**, **159**, **163**, **166**, **169**–**172**, **174**, **180**, **185** and **186** showed monophasic displacement curves.

The amino(methyl)thiazolylpropyl (**139**, **140**, **143**, **145**, **146**, **157**, **159**, **163**, **166**, **169**–**172** and **174**), aminothiazolylphenyl (**180**) and 2-amino-4,5,6,7-tetrahydrobenzothiazol-6-yl (**185** and **186**) containing ligand(s) showed a weak to moderate affinity for the hD_{2long}R (pK_i: 5.6–6.6) (Table 5). This is in contrast to the behavior at the D_3R. Apart from the weak H_2R agonists **180**, **185** and **186**, the potent H_2R ligands showed consistently high affinities at the D_3R. The two potent H_2R agonists **145** and **157** showed the highest affinity at the D_3R (pK_i: 8.21 and 8.06, respectively) (Table 5).

To obtain further information about the functional behavior of the ligands **139**, **140**, **143**, **145**, **146**, **157**, **159**, **163**, **166**, **169**–**172** and **174**, we performed the recently described β-arrestin2 recruitment assay at the hD_{2long}R and hD_3R [54]. The potencies in both assays are in very good agreement with the respective binding affinities, showing again high potencies at the D_3R (e.g. pEC_{50} (**145**): 7.81, Table 6). While the ligands appeared predominantly as moderate to strong partial agonists at the $D_{2long}R$, several full agonists at the D_3R were found (Table 6).

3. Summary and conclusions

In this study, we synthesized and characterized 49 monomeric, 2-aminothiazolyl ring-containing (thio)carbamoylguanidine-type H_2R ligands. These ligands featured either flexible or rigid spacers and were functionalized with side chains (n-alkyl, cyclic, aromatic, branched, with and without defined stereochemistry etc.) linked to the carbamoyl guanidine core. The structural simplification of previously reported dimeric ligands into monomeric ligands resulted in potent agonists (guinea pig right atrium and β-arrestin2 recruitment assays) with H_2R affinities in the one-digit nanomolar range (pK_i (**139**, UR-KAT523): 8.35; pK_i (**157**, UR-MB-69): 8.69). Most of the compounds exhibited an excellent selectivity profile towards the H_2R, for example **157** being at least 3800-fold selective within the histamine receptor family. These properties turn them into the highest affinity and subtype-selective

Table 3
gpH_2R agonism and the calculated pEC_{50} values of the monomeric (thio)carbamoylated guanidines determined by organ bath studies (spontaneously beating guinea pig right atrium).

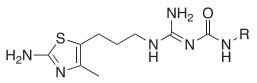

139–140, 144-160, 162, 164-165

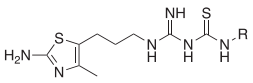

173-178

Cmpd.	R	gpH_2R (atrium)		N
		pEC_{50}	α	N
1	–	6.16 ± 0.01 [39]	1.00 [39]	225
139		8.24 ± 0.03	0.78 ± 0.03	3
140		7.80 ± 0.07	0.95 ± 0.06	3
144		7.40 ± 0.13	0.90 ± 0.06	3
145		8.12 ± 0.07	0.95 ± 0.07	4
146		7.63 ± 0.13	1.08 ± 0.07	3
147		7.32 ± 0.14	0.85 ± 0.06	3
148		7.97 ± 0.09	0.93 ± 0.04	3
149		7.46 ± 0.13	1.04 ± 0.04	3
150		7.65 ± 0.07	0.85 ± 0.05	3
151		7.63 ± 0.05	0.92 ± 0.01	3
152		7.61 ± 0.06	0.93 ± 0.04	3
153		7.26 ± 0.05	0.87 ± 0.04	3
154		7.42 ± 0.07	0.91 ± 0.04	3
155	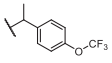	6.14 ± 0.10	0.61 ± 0.05	3
156		7.91 ± 0.01	0.93 ± 0.03	3
157		7.58 ± 0.14	0.85 ± 0.05	4
158		7.93 ± 0.07	0.58 ± 0.05	3
159		8.01 ± 0.18	1.00 ± 0.04	3
160		8.00 ± 0.05	0.88 ± 0.04	3

Table 3 (*continued*)

Cmpd.	R	gpH_2R (atrium)		N
		pEC_{50}	α	N
162		6.76 ± 0.11	0.76 ± 0.05	3
164		7.59 ± 0.05	0.99 ± 0.07	3
165		7.89 ± 0.10	0.98 ± 0.06	3
173		7.18 ± 0.10	0.67 ± 0.05	4
174		7.05 ± 0.16	0.87 ± 0.02	3
175		6.65 ± 0.14	0.65 ± 0.04	3
176		inactive	–	3
177		6.31 ± 0.05	0.44 ± 0.03	3
178		6.83 ± 0.06	0.66 ± 0.04	3

Data were analyzed by nonlinear regression and were best fitted to sigmoidal concentration response curves.pEC_{50} = -log EC_{50}.pEC_{50} was calculated from the mean-corrected shift ΔpEC_{50} of the agonist curve relative to the histamine reference ($pEC_{50} = 6.16$, N = 225) [39] curve by equation $pEC_{50} = 6.16 + \Delta pEC_{50}$.The intrinsic activity (α) of histamine was set to 1.00, and α values of investigated compounds were referred to this value. Data represent mean values ± SEM of N independent experiments.

carbamoylguanidine-type H_2R agonists known to date. On the other hand, we recognized that the 2-aminothiazole residue, which is responsible for the subtype-selectivity of monomeric and/or dimeric H_2R ligands, is also a known bioisostere of the catechol moiety present in some dopamine receptor ligands. Therefore, we investigated dopamine receptor affinity in radioligand competition binding studies at the D_{2long} and D_3 receptors with selected H_2R agonists. The experiments revealed a considerable affinity for the respective dopamine receptor subtypes, especially for the D_3 receptor. Furthermore, functional studies (β-arrestin2 recruitment assays) with these ligands showed that they act as partial and full agonists at the dopamine receptors which were investigated. These findings limit the application of our ligands to recombinant systems in which either the H_2R or the D_3R is expressed.

In summary, the aim of this work was the development of a series of H_2R agonists with enhanced drug-like properties while maintaining the high H_2R subtype selectivity and potency of the dimeric ligands. The 2-aminothiazolyl ring containing (thio)carbamoylguanidine-type H_2R ligands represent a class of high affinity molecular tools for the application in recombinant systems in which the H_2R is solely expressed. Furthermore, our ligands establish a solid base of small molecule ligands with an improved selectivity profile over previously reported ligands, enabling in vivo studies and experiments utilizing primary tissue. Consequently, the goal of future work will be the optimization of our reported compounds towards exclusive selectivity for the H_2R.

Table 4
hH_2R agonism or antagonism and the calculated pEC_{50} or pK_b values of the monomeric (thio)carbamoylated guanidines determined by a [^{35}S]GTPγS binding assay and/or β-arrestin2 recruitment assay.

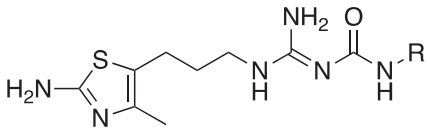

138–143, 145-146, 157, 159, 161, 163, 166-172

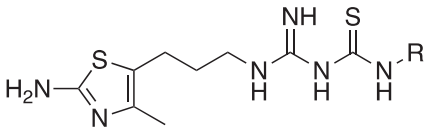

174

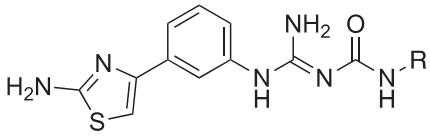

179-184

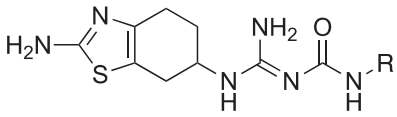

185-186

Cmpd.	R	hH_2R ([^{35}S]GTPγS)[a]			hH_2R (β-arrestin2 recruitment)[b]		
		pEC_{50} (pK_b)	N	α	pEC_{50}	N	α
1	–	6.01 ± 0.07[39]	7	1.00[39]	5.42 ± 0.02[44]	3	1.00[44]
6	–	5.07 ± 0.06	5	0.66 ± 0.08	4.40 ± 0.10	3	0.35 ± 0.03
138		6.75 ± 0.06	3	0.79 ± 0.09[c]	6.77 ± 0.04	3	0.32 ± 0.01
139		n.d.	–	n.d.	6.75 ± 0.12	3	0.15 ± 0.02
140		7.41 ± 0.07	3	0.60 ± 0.09[c]	7.07 ± 0.02	3	0.28 ± 0.03
141		6.83 ± 0.20	3	0.96 ± 0.07	6.41 ± 0.03	3	0.43 ± 0.06
142		6.28 ± 0.24	2	0.59 ± 0.02[c]	5.47 ± 0.06	3	0.25 ± 0.02
143		7.54 ± 0.12	4	0.91 ± 0.07[c]	7.00 ± 0.08	3	0.33 ± 0.03
145		n.d.	–	n.d.	7.34 ± 0.11	4	0.34 ± 0.03
146		n.d.	–	n.d.	6.48 ± 0.06	4	0.46 ± 0.02
157		n.d.	–	n.d.	7.19 ± 0.11	4	0.30 ± 0.01
159		n.d.	–	n.d.	6.63 ± 0.06	3	0.25 ± 0.01
161		7.35 ± 0.16	3	0.72 ± 0.06[c]	6.78 ± 0.03	3	0.29 ± 0.02
163		7.66 ± 0.08	3	0.65 ± 0.03[c]	6.65 ± 0.09	3	0.40 ± 0.06[c]
166		7.54 ± 0.14	3	0.60 ± 0.04	6.57 ± 0.08	3	0.16 ± 0.02[c]
167		7.51 ± 0.06	3	0.52 ± 0.03[c]	6.80 ± 0.10	3	0.11 ± 0.01[c]
168	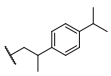	7.46 ± 0.03	3	0.59 ± 0.02[c]	6.55 ± 0.02	3	0.25 ± 0.03[c]
169		7.76 ± 0.04	3	0.60 ± 0.07	6.52 ± 0.07	3	0.22 ± 0.01[c]
170	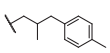	7.22 ± 0.1	5	0.68 ± 0.07[c]	6.88 ± 0.10	3	0.10 ± 0.01[c]

(*continued on next page*)

Table 4 (*continued*)

Cmpd.	R	hH_2R ([^{35}S]GTPγS)[a]			hH_2R (β-arrestin2 recruitment)[b]		
		pEC_{50} (pK_b)	N	α	pEC_{50}	N	α
171	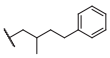	7.53 ± 0.06	3	0.69 ± 0.02[c]	6.45 ± 0.06	3	0.20 ± 0.02[c]
172	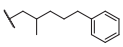	n.d.	–	n.d.	5.60 ± 0.11	4	0.14 ± 0.02
174		n.d.	–	n.d.	6.43 ± 0.06	3	0.11 ± 0.01
179		(4.91 ± 0.09)	3	n.d.	n.d.	–	n.d.
180		(6.14 ± 0.03)	3	n.d.	n.d.	–	n.d.
181		(5.40 ± 0.02)	3	n.d.	n.d.	–	n.d.
182		(4.76 ± 0.11)	3	n.d.	n.d.	–	n.d.
183		(5.44 ± 0.02)	3	n.d.	n.d.	–	n.d.
184		(5.52 ± 0.05)	3	n.d.	n.d.	–	n.d.
185		6.83 ± 0.06	3	0.16 ± 0.07[c]	n.d.	–	n.d.
186		6.67 ± 0.31	3	0.53 ± 0.05[c]	5.36 ± 0.05	3	0.31 ± 0.03

[a][^{35}S]GTPγS assay performed with membrane preparations of Sf9 insect cells expressing the hH_2R-$G_{s\alpha S}$ fusion protein [14,39,42,43]. [b]β-arrestin2 recruitment determined using HEK293T-β-Arr2-hH_2R cells, stably expressing the hH_2R-ElucC and βArr2-ElucN fusion constructs [43–45]. The intrinsic activity (α) of histamine was set to 1.00, and the α values of investigated compounds were referred to this value. The pK_b values of **179**–**184** were determined in the antagonist mode versus histamine (c = 1 μM). Data represent mean values ± SEM of N independent experiments, each performed in triplicate ([^{35}S]GTPγS assay) or duplicate/triplicate (β-arrestin2 recruitment assay). n.d.: not determined. [c]At concentrations ≥ 30 μM a varying degree of depression of the maximum effect was observed. This effect has already been reported for several GPCRs in the literature [46–52].

4. Experimental section

4.1. General

Unless otherwise stated, chemicals and solvents were procured from commercial suppliers and used as received. All the solvents were of analytical grade or distilled prior to use. Anhydrous solvents were stored over molecular sieve under protective gas. Deuterated solvents for nuclear magnetic resonance (NMR) spectroscopy were purchased from Deutero (Kastellaun, Germany). For the preparation of buffers and HPLC eluents Millipore-grade water was used. Column chromatography was carried out using silica gel 60 (0.040–0.063 mm, Merck (Darmstadt, Germany)). Automated flash chromatography was performed with an IntelliFlash-310 flash-purification system (Varian, Darmstadt, Germany) with pre-packed columns (SuperFlash SF10-4 g, SF12-8 g, SF15-12 g und SF15-24 g, Agilent Technologies, Santa Clara, CA). Reactions were monitored by thin layer chromatography (TLC) on silica gel 60 F254 aluminium sheets (Merck), and compounds were detected with UV light at 254 nm and ninhydrin solution (0.8 g ninhydrin, 200 mL n-butanol, 6 mL acetic acid). NMR spectra (^{1}H NMR and ^{13}C NMR, ^{19}F NMR, DEPT, 2D NMR) were recorded on a Bruker Avance-300 (7.05 T, ^{1}H: 300 MHz, ^{13}C: 75.5 MHz, ^{19}F: 188), Avance-400 (9.40 T, ^{1}H: 400 MHz, ^{13}C: 100.6 MHz, ^{19}F: 282), or Avance-600 (14.1 T; ^{1}H: 600 MHz, ^{13}C: 150.9 MHz; cryogenic probe) NMR spectrometer (Bruker, Karlsruhe, Germany). Multiplicities are specified with the following abbreviations: s (singlet), d (doublet), t (triplet), q (quartet), quint (quintet), m (multiplet), br (broad), as well as combinations thereof. High-resolution mass spectrometry (HRMS) was performed on an AccuTOF GCX GC/MS system (Jeol, Peabody, MA, USA) using an EI source or a Q-TOF 6540 UHD LC or GC/MS system (Agilent Technologies, Santa Clara, USA) using an ESI (in case of LC coupling) or an APCI (in case of GC coupling) source. Optical rotations at 589 nm (Na D line) were measured on a polarimeter P8000-T equipped with an electronic Peltier thermostat PT31 (A. KRÜSS Optronic, Hamburg, Germany) using a thermostated (20 °C) microcuvette (layer thickness of 1 dm, volume of 0.9 mL) and methanol (MeOH) as solvent. Preparative HPLC was performed with a system from Knauer (Berlin, Germany) consisting of two K-1800 pumps and a K-2001 detector or with a Prep 150 LC system from Waters (Eschborn, Germany) consisting of a 2545 binary gradient module, a 2489 UV/visible detector and a fraction collector III. The following columns were used: a Nucleodur 100-5 C18 (5 μm, 250 × 21 mm, Macherey-Nagel, Düren, Germany), a Kinetex XB-C18 100A (5 μm, 250 × 21.2 mm, Phenomenex, Aschaffenburg, Germany), an Interchim PuriFlash PF15C18 HQ (15 μm, 120 g, Interchim, Montluçon, France) and a Gemini-NX C18 (5 μm, 250 mm × 21 mm; Phenomenex). Solvent flow rates of either 15–20 mL/min (Nucleodur, Kinetex and Gemini columns) or 30 mL/min (Interchim column) at rt were employed. A detection wavelength of 220 nm and mixtures of acetonitrile (MeCN) and 0.05–0.1% aqueous TFA were used as mobile phases. MeCN was removed from the eluates under reduced pressure prior to freeze-drying (Christ Alpha 2–4 LD freeze dryer (Martin Christ, Osterode am Harz, Germany) or ScanVac CoolSafe 4–15L freeze dryer from Labogene (LMS, Brigachtal, Germany), both equipped with a RZ 6 rotary vane vacuum pump (Vacuubrand, Wertheim, Germany)). Analytical HPLC analysis was performed on a system from Merck Hitachi, composed of a D-6000 interface, a L-6200A pump, an AS2000A auto sampler and a L-4000 UV-VIS detector or with a 1100 HPLC system from Agilent technologies, equipped with an Instant Pilot controller, a G1312A binary pump, a G1329A ALS autosampler,

Table 5
Affinities of the monomeric (thio)carbamoylated guanidines to the dopamine receptors $hD_{2long}R$ and hD_3R, obtained from competition binding studies.

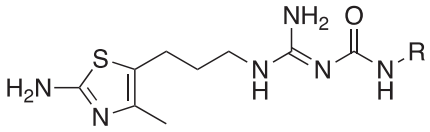

139–140, 143, 145-146, 157, 159, 163, 166, 169-172

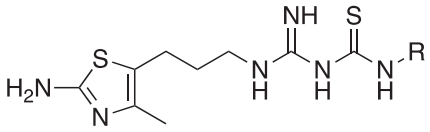

174

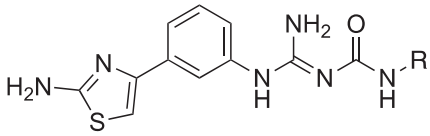

180

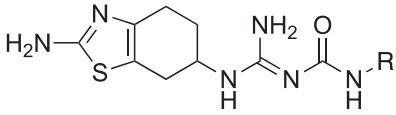

185-186

Cmpd.	R	pK_i				Selectivity ratios of K_i ($D_{2long}R/D_3R/H_2R$)
		$hD_{2long}R$[a]	N	hD_3R[b]	N	
haloperidol		9.58 ± 0.13 [54]	3	8.95 ± 0.03 [54]	3	–
6		(p$K_{i/high}$: 7.59 ± 0.12/p$K_{i/low}$: 6.00 ± 0.03) [54]	3	9.18 ± 0.06 [54]	3	0.002*/0.00005/1
139		6.35 ± 0.01	3	7.80 ± 0.09	3	100/4/1
140		6.25 ± 0.06	3	7.85 ± 0.08	3	19/0.5/1
143		6.22 ± 0.08	3	7.34 ± 0.02	3	9/0.7/1
145		6.81 ± 0.13	3	8.21 ± 0.10	3	9/0.3/1
146		6.10 ± 0.07	3	7.61 ± 0.12	3	15/0.5/1
157		6.50 ± 0.06	3	8.06 ± 0.10	3	155/4/1
159		5.77 ± 0.12	3	7.76 ± 0.17	3	54/0.5/1
163		6.58 ± 0.03	3	7.36 ± 0.04	3	7/1/1
166		6.28 ± 0.08	3	7.19 ± 0.06	3	7/0.8/1
169		6.32 ± 0.08	3	6.88 ± 0.04	3	7/2/1
170	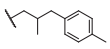	6.30 ± 0.10	3	7.07 ± 0.06	3	7/1/1
171	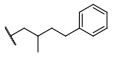	6.45 ± 0.07	3	7.34 ± 0.04	3	6/0.7/1
172	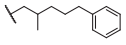	6.23 ± 0.06	3	7.25 ± 0.06	3	10/0.9/1
174		5.93 ± 0.08	3	7.22 ± 0.06	3	10/0.5/1
180		5.60 ± 0.20	3	5.89 ± 0.05	3	4/2/1
185		5.90 ± 0.10	3	5.90 ± 0.20	3	1/1/1
186		6.26 ± 0.10	3	5.30 ± 0.10	3	1/10/1

Determined by displacing [^{3}H]*N*-methylspiperone ([a]$hD_{2long}R$: K_d = 0.0149 nM, c = 0.05 nM or [b]hD_3R: K_d = 0.0258 nM, c = 0.05 nM) by increasing concentrations of the respective ligand at homogenates of [a]HEK293T-CRE-Luc-$hD_{2long}R$ or [b]HEK293T-CRE-Luc-hD_3R cells [54]. Data were analyzed by nonlinear regression and were best fitted to four-parameter sigmoidal concentration-response curves. Data shown are means ± SEM of N independent experiments, each performed in triplicate.*Calculated using p$K_{i/high}$ value.

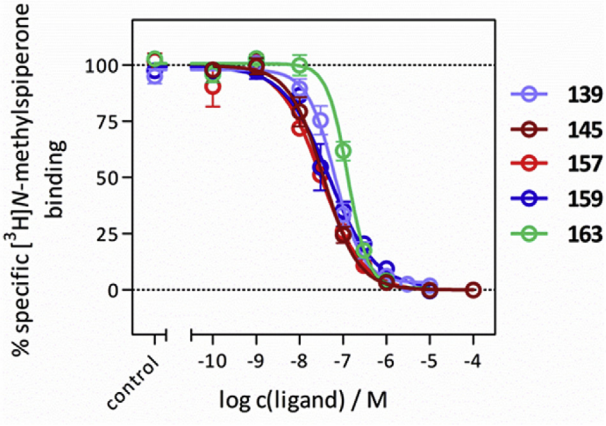

Fig. 4. Displacement of the radioligand [^{3}H]*N*-methylspiperone (c = 0.05 nM, K_d = 0.0258 nM) by increasing concentrations of the respective ligand at homogenates of HEK293T-CRE-Luc-hD$_3$R cells [54]. Data represent mean values ± SEM of 3 independent experiments, each performed in triplicate.

a G1379A vacuum degasser, a G1316A column compartment and a G1315B DAD detector. A Kinetex XB-C18 100A (5 μm, 250 × 4.6 mm (Phenomenex)) served as the column: t_0 = 2.90 min (Merck Hitachi, flow: 0.8 mL/min), t_0 = 3.16 min (Merck Hitachi, flow: 0.8 mL/min, different Kinetex XB-C18 100A column), t_0 = 2.85 min (Merck Hitachi, flow: 1.0 mL/min, different Kinetex XB-C18 100A column), t_0 = 3.21 min (Agilent, flow: 0.8 mL/min) or t_0 = 2.67 min (Agilent, flow: 1.0 mL/min). As the mobile phase, mixtures of MeCN (with (A) or without (B) 0.05% TFA) and 0.05% aqueous TFA (C) were used. The following linear gradients were applied. Compounds **179**–**180** and **182**–**186** (Merck Hitachi, t_0 = 2.90 min): 0–30 min: A/C 5:95–80:20; 30–32 min: 80:20–95:5; 32–42 min: 95:5; flow rate: 0.8 mL/min. Compounds **138**, **140**–**143**, **161**, **163**, **166**–**171** and **181** (Merck Hitachi, t_0 = 2.90 min): 0–30 min: A/C 10:90–80:20; 30–32 min: 80:20–95:5; 32–42 min: 95:5; flow rate: 0.8 mL/min. Compounds **144**–**146**, **162**, **164**–**165** and **173**–**178** (Merck Hitachi, t_0 = 3.16 min): 0–25 min: B/C 20:80–80:20; 25–26 min: 80:20–95:5; 26–35 min: 95:5; flow rate: 0.8 mL/min. Compounds **149** (Merck Hitachi, t_0 = 2.85 min): 0–25 min: B/C 5:95–95:5; 25–35 min: 95:5; flow rate: 1.0 mL/min. Compounds **139** and **172** (Agilent, t_0 = 3.21 min): 0–30 min: B/C 10:90–90:10; 30–33 min: 90:10–95:5; 33–40 min: 95:5; flow rate: 0.8 mL/min. Compounds **147**–**148** and **150**–**160** (Agilent, t_0 = 2.67 min): 0–25 min: B/C 10:90–95:5; 25–35 min: 95:5; flow rate: 1.0 mL/min. For analytical HPLC runs on the 1100 HPLC system from Agilent Technologies the oven temperature was set to 30 °C. At the HPLC system from Merck Hitachi room temperature was used. The injection volume was 5–100 μL, and detection was performed at 220 nm. Compound concentrations were between 0.1 and 1 mM.

Compounds purities were calculated as the percentage peak area of the analyzed compound by UV detection at 220 nm. The purities of the target compounds **139**–**186** used for pharmacological investigation were ≥ 95% (chromatograms shown in the SM, Figs. S24–S72).

4.2. Synthesis and analytical data

4.2.1. General procedure for the synthesis of the Boc-protected isothioureas 48-82

Method A: A solution of 15% phosgene in toluene or triphosgene (1 equiv) was diluted in DCM and cooled to 0 °C. Subsequently, a mixture of the respective amine (**13**–**33**, 1 equiv) and diisopropylethylamine (DIPEA, 3 equiv) in DCM was added dropwise. After the solution was stirred for 5-30 min, a solution of **8** (2 equiv) in DCM was added via a dropping funnel. The reaction was allowed to stir at rt for 2–3 h and washed with H_2O and brine. The organic layer was dried over Na_2SO_4, the solvent was removed under reduced pressure and the crude product was purified by column chromatography (DCM).

Method B: The respective isocyanate (**34**–**39**, 1 equiv) and TEA (2.25 equiv) were added to a solution of **8** (1.5 equiv) in DCM (20 mL). The reaction mixture was stirred overnight at rt. The organic layer was washed three times with H_2O (30 mL) and subsequently with brine (30 mL). The organic layer was dried over Na_2SO_4 and the solvent was removed under reduced pressure. The crude product was purified by flash chromatography (ethyl acetate (EtOAc)/petroleum ether (PE) 0/100 - 15/85).

Method C: The respective carbonic acid (**40**–**47**, 1 equiv) was dissolved in DCM (2.5–4.5 mL) and cooled with an ice bath. Dimethylformamide (DMF, 25–45 μL) and oxalyl chloride (1.5 equiv) were added under argon atmosphere. The reaction mixture was stirred for 10 min under cooling. The ice bath was removed and stirring was continued for another 15 min at rt. The solvent was carefully removed under reduced pressure (water bath temperature below 30 °C). The residue was dissolved in anhydrous acetone (2.5–4.5 mL) and added dropwise under cooling to an ice-cold solution of sodium azide (2.4 equiv) in H_2O (1–3 mL). The reaction mixture was stirred for 30 min under cooling. Brine (5–10 mL) was added and the acyl azide was extracted three times with DCM (10 mL). The organic layers were combined and dried over Na_2SO_4. Molecular sieve was added and the solvent was partially removed under reduced pressure. The resulting yellow solution was stirred for 30 min under reflux conditions to afford the isocyanate. The solution was cooled to rt followed by the addition of **8** (1 equiv) and TEA (5 equiv). The reaction mixture was stirred overnight at rt. The molecular sieve was filtered off and the organic layer was washed three times with H_2O (10 mL) and three times with brine (10 mL). The organic layers were combined, dried over Na_2SO_4 and the solvent was removed under reduced pressure. The crude product was purified by either automated flash chromatography or column chromatography (EtOAc/PE).

4.2.2. N′-tert-butoxycarbonyl-S-methyl-N-pentylcarbamoylisothiourea (49)

The reaction was carried out with triphosgene (340 mg, 1.15 mmol), pentan-1-amine (**14**, 132 μL, 1.15 mmol), DIPEA (0.60 mL, 3.45 mmol), **8** (0.44 g, 2.30 mmol) and a total of 60 mL DCM according to the general procedure (method A) (R_f = 0.64 in EtOAc/PE 1/5) yielding a colorless foamlike solid (0.30 g, 84%). ^{1}H NMR (300 MHz, $CDCl_3$): δ (ppm) 12.27 (br s, 1H), 5.51 (s, 1H), 3.15 (q, J = 6.72 Hz, 2H), 2.23 (s, 3H), 1.58–1.42 (m, 2H), 1.41 (s, 9H), 1.34–1.19 (m, 4H), 0.91–0.75 (m, 3H). ^{13}C NMR (75 MHz, $CDCl_3$): δ (ppm) 167.31, 162.05, 151.27, 82.64, 40.28, 29.53, 29.22, 28.16, 22.52, 14.39, 14.13. HRMS (ESI-MS): m/z [M + H$^+$] calculated for $C_{13}H_{26}N_3O_3S^+$: 304.1689, found 304.1713; $C_{13}H_{25}N_3O_3S$ (303.42).

4.2.3. (R)-N′-tert-butoxycarbonyl-S-methyl-N-(1-phenylethyl) carbamoylisothiourea (55)

The reaction was carried out with 15% phosgene in toluene (5.89 mL, 8.25 mmol), (R)-1-phenylethan-1-amine (**15**, 1.00 g, 8.25 mmol), DIPEA (4.46 mL, 24.75 mmol), **8** (3.14 g, 16.50 mmol) and a total of 150 mL DCM according to the general procedure (method A) (R_f = 0.50 in DCM) yielding a colorless foamlike solid (1.60 g, 57%). ^{1}H NMR (300 MHz, $CDCl_3$) δ (ppm) 12.29 (br s, 1H), 7.41–7.26 (m, 5H), 5.81 (br s, 1H), 4.93 (quint, J = 7.1 Hz, 1H), 2.32 (s, 3H), 1.52 (d, J = 6.9 Hz, 3H), 1.46 (s, 9H). ^{13}C NMR (75 MHz, $CDCl_3$) δ (ppm) 167.92, 161.02, 151.13, 143.44, 128.75, 127.39, 125.98, 82.67, 49.79, 28.04, 22.31, 14.38. HRMS (ESI-MS): m/z [M + H$^+$] calculated

Table 6
$hD_{2long,3}R$ agonism and the calculated pEC_{50} values of the monomeric (thio)carbamoylated guanidines determined by a β-arrestin2 recruitment assay.

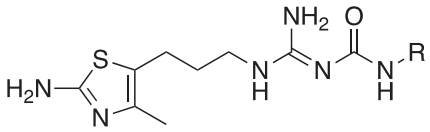

139–140, 143, 145-146, 157, 159, 163, 166, 169-172

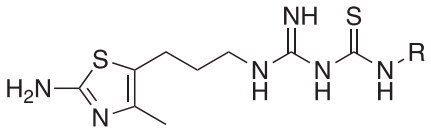

174

Cmpd.	R	$hD_{2long}R$ (β-arrestin2 recruitment)[a]			hD_3R (β-arrestin2 recruitment)[b]		
		pEC_{50}	N	α	pEC_{50}	N	α
quinpirole	–	7.55 ± 0.07 [54]	5	1.00 [54]	8.75 ± 0.07 [54]	6	1.00 [54]
139		5.98 ± 0.02	4	0.41 ± 0.05	7.80 ± 0.05	3	0.96 ± 0.05
140		5.76 ± 0.06	3	0.44 ± 0.05	7.63 ± 0.12	4	0.95 ± 0.05
143		5.78 ± 0.05	3	0.49 ± 0.03	7.47 ± 0.08	3	0.93 ± 0.03
145		6.47 ± 0.10	4	0.60 ± 0.05	7.81 ± 0.03	4	0.86 ± 0.05
146		5.57 ± 0.28	3	0.36 ± 0.04	6.64 ± 0.07	3	1.05 ± 0.09
157		6.23 ± 0.10	3	0.73 ± 0.05	7.14 ± 0.16	3	0.98 ± 0.05
159		5.97 ± 0.09	3	0.82 ± 0.03	6.99 ± 0.09	3	1.03 ± 0.10
163		5.49 ± 0.15	4	0.39 ± 0.06	6.58 ± 0.05	3	1.09 ± 0.09
166		5.95 ± 0.04	3	0.58 ± 0.02	7.39 ± 0.08	3	0.93 ± 0.04
169		5.77 ± 0.04	3	0.57 ± 0.02	6.52 ± 0.02	3	0.86 ± 0.01
170	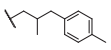	5.96 ± 0.05	5	0.92 ± 0.10	6.55 ± 0.13	3	1.01 ± 0.07
171	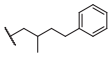	5.27 ± 0.07	3	0.70 ± 0.08	6.05 ± 0.11	3	0.95 ± 0.11
172	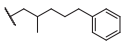	5.53 ± 0.02	3	0.70 ± 0.11	6.38 ± 0.10	3	0.67 ± 0.06
174		5.82 ± 0.06	3	0.66 ± 0.08	6.78 ± 0.09	3	0.84 ± 0.04

β-arrestin2 recruitment determined using [a]HEK293T ElucN-βarr2 $hD_{2long}R$-ElucC cells or [b]HEK293T ElucN-βarr2 hD_3R-ElucC cells, stably expressing the $hD_{2long}R$-ElucC or hD_3R-ElucC and βarr2-ElucN fusion constructs [54]. The intrinsic activity (α) of quinpirole was set to 1.00, and α values of investigated compounds were referred to this value. Data represent mean values ± SEM of 3–4 independent experiments, each performed in duplicate or triplicate.

for $C_{16}H_{24}N_3O_3S^+$: 338.1533, found 338.1542; $C_{16}H_{23}N_3O_3S$ (337.44).

4.2.4. *N′-tert-butoxycarbonyl-S-methyl-N-(1-(3-fluorophenyl) ethyl)carbamoylisothiourea (67)*

The reaction was carried out with 15% phosgene in toluene (3.08 mL, 4.31 mmol), **27**-HCl (0.60 g, 4.31 mmol), DIPEA (2.20 mL, 12.93 mmol), **8** (1.64 g, 8.62 mmol) and a total of 100 mL DCM according to the general procedure (method A) ($R_f = 0.76$ in DCM) yielding a colorless oil (0.77 g, 51%). ^{1}H NMR (400 MHz, $CDCl_3$) δ (ppm) 12.40 (s, 1H), 7.48–7.02 (m, 4H), 6.16 (d, $J = 7.8$ Hz, 1H), 5.06 (quint, $J = 7.1$ Hz, 1H), 2.44 (s, 3H), 1.61 (d, $J = 7.5$ Hz, 2H), 1.60 (s, 9H). ^{13}C NMR (101 MHz, $CDCl_3$) δ (ppm) 162.96 (d, $J = 246.2$ Hz), 161.64, 161.01, 150.93, 146.32 (d, $J = 6.6$ Hz), 130.14 (d, $J = 8.2$ Hz), 121.55 (d, $J = 2.8$ Hz), 114.04 (d, $J = 21.1$ Hz), 112.80 (d, $J = 21.8$ Hz), 82.55, 53.14, 27.89, 22.15, 14.42. HRMS (ESI-MS): *m/z* $[M + H^+]$ calculated for $C_{16}H_{23}FN_3O_3S^+$: 356.1439, found 356.1445; $C_{16}H_{22}FN_3O_3S$ (355.43).

4.2.5. *General procedure for the synthesis of the isothiocyanates 83-88*

A solution of the respective amine (**14**–**16** or **31**–**33**, 1 equiv) in DCM was added to a saturated solution of $NaHCO_3$ at rt. Subsequently, thiophosgene (1.1 equiv) was added dropwise and the reaction was stirred vigorously for 30 min at rt. The organic layer was washed with H_2O, brine and dried over Na_2SO_4. The solvent

was removed under reduced pressure and the crude product was purified with column chromatography (EtOAc/PE 5/95).

4.2.6. (R)-(1-Isothiocyanatoethyl)benzene (84)

The product was prepared from (R)-1-phenylethan-1-amine (**15**, 0.21 g, 1.71 mmol) and thiophosgene (144 μL, 1.88 mmol) in DCM (20 mL) and a saturated solution of $NaHCO_3$ (20 mL) according to the general procedure (R_f = 0.63 in EtOAc/PE 5/95). The desired compound **84** was isolated as an orange oil (0.17 g, 61%). ^{1}H NMR (300 MHz, $CDCl_3$) δ (ppm) 7.44–7.29 (m, 5H), 4.92 (q, J = 6.8 Hz, 1H), 1.68 (d, J = 6.8 Hz, 3H). ^{13}C NMR (75 MHz, $CDCl_3$) δ (ppm) 140.18, 132.30, 128.95, 128.25, 125.46, 57.07, 25.03. HRMS (EI-MS): m/z [$M^{\bullet+}$] calculated for $C_9H_9NS^{\bullet+}$: 163.0450, found 163.0454; C_9H_9NS (163.24).

4.2.7. General procedure for the guanidinylation reaction of 89–123 and 130-137

The general procedure for the synthesis of **89**–**123** and **130**–**137** is described in the literature [14,55]. The precursor amine **9a** was synthesized as described by Kraus et al. [11] For the synthesis of precursor amines **9b**, **11** and **12** see in the SM (Schemes S1 and S2). The compounds **89**–**94**, **112**, **114**, **117**–**123** and **130**–**137** were directly Boc- or Trt-deprotected as described in the general procedure for the preparation of the title compounds without analytical characterization of the Boc-/Trt-protected intermediates. The used amounts of the respective substrates and reagents are described in the characterization of **138**–**143**, **161**, **163**, **166**–**172** and **179**–**186**, respectively.

4.2.8. (R)-1-(tert-Butoxycarbonylamino((3-(2-tert-butoxycarbonylamino-4-methylthiazol-5-yl)propyl)amino) methylene)-3-(1-phenylethyl)urea (96)

Compound **96** was prepared from **9a** (1.29 g, 4.75 mmol), **55** (1.60 g, 4.75 mmol), $HgCl_2$ (1.29 g, 4.75 mmol) and TEA (1.98 mL, 14.25 mmol) in DCM (50 mL) conforming to the general procedure (R_f = 0.45 in DCM/MeOH/NH_3 99/1/0.1) yielding a yellow oil (2.02 g, 76%). ^{1}H NMR (300 MHz, $CDCl_3$) δ (ppm) 12.08 (br s, 1H), 10.33 (br s, 1H), 8.12 (br s, 1H), 7.42–7.13 (m, 5H), 5.59 (br s, 1H), 4.91 (quint, J = 7.1 Hz, 1H), 3.35 (q, J = 6.6 Hz, 2H), 2.71 (t, J = 7.3 Hz, 2H), 2.23 (s, 3H), 1.87 (quint, J = 7.2 Hz, 2H), 1.51 (s, 9H), 1.47 (d, J = 7.0 Hz, 3H), 1.44 (s, 9H). ^{13}C NMR (75 MHz, $CDCl_3$) δ (ppm) 163.84, 157.50, 154.45, 153.42, 152.69, 144.52, 142.00, 128.57, 126.95, 125.92, 123.25, 82.45, 82.22, 49.57, 39.61, 30.76, 28.27, 28.06, 23.27, 22.81, 14.54. HRMS (ESI-MS): m/z [M + H^+] calculated for $C_{27}H_{41}N_6O_5S^+$: 561.2854, found 561.2863; $C_{27}H_{40}N_6O_5S$ (560.71).

4.2.9. 1-(tert-Butoxycarbonylamino((3-(2-tert-butoxycarbonylamino-4-methylthiazol-5-yl)propyl)amino) methylene)-3-(1-(3-fluorophenyl)ethyl)urea (108)

Compound **108** was prepared from **9a** (0.32 g, 1.19 mmol), **67** (0.42 g, 1.19 mmol), $HgCl_2$ (0.32 g, 1.19 mmol) and TEA (0.50 mL, 3.58 mmol) in DCM (10 mL) conforming to the general procedure (R_f = 0.12 in DCM/MeOH/NH_3 99/1/0.1) yielding a colorless oil (0.21 g, 36%). ^{1}H NMR (400 MHz, $CDCl_3$) δ (ppm) 12.02 (s, 1H), 10.25 (s, 1H), 8.18 (s, 1H), 7.32–6.84 (m, 4H), 5.67 (s, 1H), 4.89 (quint, J = 7.1 Hz, 1H), 3.43–3.30 (m, 2H), 2.71 (t, J = 7.3 Hz, 2H), 2.22 (s, 3H), 1.88 (quint, J = 7.1 Hz, 2H), 1.50 (s, 9H), 1.46 (d, J = 3.5 Hz, 3H), 1.44 (s, 9H). ^{13}C NMR (101 MHz, $CDCl_3$) δ (ppm) 163.03 (d, J = 245.7 Hz), 157.54, 154.57, 153.36, 147.43 (d, J = 6.5 Hz), 141.88, 130.02 (d, J = 8.2 Hz), 123.17, 121.49 (d, J = 2.7 Hz), 113.73 (d, J = 21.2 Hz), 112.79 (d, J = 21.8 Hz), 82.61, 82.20, 49.22, 41.01, 30.73, 28.24, 28.04, 23.22, 22.74, 14.47. HRMS (ESI-MS): m/z [M + H^+] calculated for $C_{27}H_{40}FN_6O_5S^+$: 579.2759, found 579.2775; $C_{27}H_{39}FN_6O_5S$ (578.70).

4.2.10. General procedure of the thiocarbamoylation (124–129)

The Boc-protected guanidine **10** (1 equiv; synthesized as described by Kraus et al. [11]) and the respective isothiocyanate **83**–**88** (1 equiv) were dissolved in DCM and refluxed for 3–4 days. After the reaction was complete (TLC monitoring), the solvent was evaporated and the crude product was purified by column chromatography (DCM/MeOH 100/0–98/2). The NMR peaks in the ^{1}H and ^{13}C NMR are split due to thione-thiol tautomerism, as already described in the literature [55]. For ^{1}H NMR each pair of peaks was integrated jointly. For ^{13}C NMR just one peaks series was taken and described.

4.2.11. (R)-1-(tert-Butoxycarbonylamino((3-(2-tert-butoxycarbonylamino-4-methylthiazol-5-yl)propyl)amino) methylene)-3-(1-phenylethyl)thiourea (125)

The title compound was prepared from **10** (0.12 g, 0.28 mmol) and **84** (0.05 g, 0.28 mmol) in DCM (10 mL) according to the general procedure (R_f = 0.48 in DCM/MeOH 99/1). **125** was yielded as yellow oil (50 mg, 31%). ^{1}H NMR (300 MHz, $CDCl_3$) δ (ppm) 13.00 (s, 1H), 10.48 (br s, 1H), 8.48 (t, J = 5.7 Hz, 1H), 7.38–7.26 (m, 5H), 6.65 (d, J = 7.0 Hz, 1H), 5.16 (q, J = 7.0 Hz, 1H), 3.21–3.06 (m, 2H), 2.55 (q, J = 7.5 Hz, 2H), 2.19 (s, 3H), 1.91–1.79 (m, 2H), 1.51 (s, 9H), 1.51 (s, 3H), 1.47 (s, 9H). ^{13}C NMR (75 MHz, $CDCl_3$) δ (ppm) 183.54, 157.65, 154.85, 153.71, 153.40, 152.74, 143.87, 128.52, 126.47, 125.61, 122.91, 83.30, 82.29, 53.28, 39.69, 30.46, 29.72, 28.29, 28.03, 22.73, 14.49. HRMS (ESI-MS): m/z [M + H^+] calculated for $C_{27}H_{41}N_6O_4S_2^+$: 577.2625, found 577.2631; $C_{27}H_{40}N_6O_4S_2$ (576.78).

4.2.12. General procedure for the Boc-/Trt-deprotection to obtain the title compounds 138–172 and 179-186

The general procedure for the synthesis of **138**–**172** and **179**–**186** by Boc-/Trt-deprotection is described in the literature [14,39,55]. All compounds, with exception of **149** and **155**, were purified by preparative HPLC (MeCN/0.05 or 0.1% aqueous TFA and obtained as di-trifluoroacetates (method A). **149** and **155** were purified as follows: The crude product was subjected to column chromatography under basic conditions (DCM/MeOH/NH_3 90/10/0.1). The free base was dissolved in 2–3 mL dioxane and precipitated after dropwise addition of 2 N HCl in diethyl ether. The resulting dihydrochloride was separated and washed with diethyl ether (3 × 5 mL) (method B).

4.2.13. 1-(Amino((3-(2-amino-4-methylthiazol-5-yl)propyl)amino) methylene)-3-(1-pentyl)urea (139)

90 was prepared from **9a** (0.05 g, 0.17 mmol), **49** (0.05 g, 0.17 mmol), $HgCl_2$ (0.09 g, 0.34 mmol) and TEA (0.07 mL, 0.51 mmol) in DCM (25 mL) conforming to the general procedure for the guanidinylation reaction. Subsequently, **139** was prepared from the Boc-protected intermediate **90** in DCM (4.0 mL) and TFA (1.0 mL) according to the general procedure (method A) and obtained as a colorless foamlike solid (140 mg, 49%): RP-HPLC: 99%, (t_R = 11.14, k = 2.47). ^{1}H NMR (600 MHz, DMSO-d_6, di-trifluoroacetate) δ (ppm) 10.46 (s, 1H), 9.40–8.79 (m, 3H), 8.52 (s, 2H), 7.48 (s, 1H), 3.24 (q, J = 6.6 Hz, 2H), 3.09 (q, J = 6.6 Hz, 2H), 2.59 (t, J = 7.5 Hz, 2H), 2.08 (s, 3H), 1.73 (quint, J = 7.3 Hz, 2H), 1.43 (quint, J = 7.2 Hz, 2H), 1.32–1.19 (m, 4H), 0.86 (t, J = 7.1 Hz, 3H). ^{13}C NMR (151 MHz, DMSO-d_6, di-trifluoroacetate) δ (ppm) 167.82, 159.12 (q, J = 32.4 Hz, TFA), 153.83, 153.69, 131.95, 116.89 (q, J = 298.1 Hz, TFA), 116.28, 39.93, 39.16, 28.82, 28.59, 28.37, 21.98, 21.74, 13.86, 11.44. HRMS (ESI-MS): m/z [M + H^+] calculated for $C_{14}H_{27}N_6OS^+$: 327.1962; found 327.1964; $C_{14}H_{26}N_6OS$ x 2 TFA (554.51).

4.2.14. (R)-1-(Amino((3-(2-amino-4-methylthiazol-5-yl)propyl) amino)methylene)-3-(1-phenylethyl)urea (145)

145 was prepared from **96** (2.02 g, 3.60 mmol) in DCM (16.0 mL)

and TFA (4.0 mL) according to the general procedure (method A) and obtained as a colorless foamlike solid (210 mg, 74%): RP-HPLC: 99%, (t_R = 11.14, k = 2.53), ee = 99%, [α] $^{20}_D$ +26.54 (c 0.31, MeOH). ^{1}H NMR (300 MHz, CD_3OD, di-trifluoroacetate) δ (ppm) 7.59–6.96 (m, 5H), 4.88–4.84 (m, 1H), 3.34–3.25 (m, 2H), 2.69 (t, J = 7.5 Hz, 2H), 2.16 (s, 3H), 1.87 (quint, J = 7.1 Hz, 2H), 1.47 (d, J = 7.0 Hz, 3H). ^{13}C NMR (75 MHz, CD_3OD, di-trifluoroacetate) δ (ppm) 170.38, 155.99, 154.73, 144.89, 132.62, 129.68, 128.38, 127.03, 118.40, 51.17, 41.44, 29.89, 23.58, 22.70, 11.45. HRMS (ESI-MS): m/z [M + H$^+$] calculated for $C_{17}H_{25}N_6OS^+$: 361.1805, found 361.1802; $C_{17}H_{24}N_6OS$ x 2 TFA (588.53).

4.2.15. 1-(Amino((3-(2-amino-4-methylthiazol-5-yl)propyl)amino) methylene)-3-(1-(3-fluorophenyl)ethyl)urea (157)

157 was prepared from **108** (0.21 g, 0.36 mmol) in DCM (8.0 mL) and TFA (2.0 mL) according to the general procedure (method A) and obtained as a colorless foamlike solid (100 mg, 45%): RP-HPLC: 99%, (t_R = 9.50, k = 2.56). ^{1}H NMR (400 MHz, CD_3OD, di-trifluoroacetate) δ (ppm) 7.38–7.28 (m, 1H), 7.16–6.94 (m, 3H), 4.91 (q, 1H), 2.69 (t, J = 7.6 Hz, 2H), 2.15 (s, 3H), 1.94–1.81 (m, 2H), 1.47 (d, J = 7.0 Hz, 3H). ^{13}C NMR (101 MHz, CD_3OD, di-trifluoroacetate) δ (ppm) 168.92, 162.98 (d, J = 244.6 Hz), 162.07 (q, J = 34.6 Hz, TFA), 154.54, 153.34, 146.50 (d, J = 6.8 Hz), 131.26, 129.98 (d, J = 8.2 Hz), 121.44 (d, J = 2.9 Hz), 116.95, 116.59 (q, J = 291.7 Hz, TFA), 113.50 (d, J = 21.3 Hz), 112.42 (d, J = 22.2 Hz), 49.34 (d, J = 1.2 Hz), 48.03, 40.00, 28.43, 22.13, 21.03, 10.02. ^{19}F NMR (377 MHz, CD_3OD, di-trifluoroacetate) δ (ppm) −75.42 (TFA), −113.47. HRMS (ESI-MS): m/z [M + H$^+$] calculated for $C_{17}H_{24}FN_6OS^+$: 379.1711, found 379.1711; $C_{17}H_{23}FN_6OS$ x 2 TFA (606.52).

4.2.16. (R)-1-(Amino((3-(2-amino-4-methylthiazol-5-yl)propyl) amino)methylene)-3-(1-phenylethyl)thiourea (174)

174 was prepared from **125** (0.05 g, 0.09 mmol) in DCM (4.0 mL) and TFA (1.0 mL) according to the general procedure and obtained as a colorless solid (30 mg, 57%), mp 75–78 °C, RP-HPLC: 95%, (t_R = 14.18, k = 3.49), ee = 99%, [α]$^{20}_D$ +20.30 (c 0.34, MeOH). ^{1}H NMR (300 MHz, CD_3OD, di-trifluoroacetate) δ (ppm) 7.42–7.19 (m, 5H), 5.45 (q, J = 7.5, 7.0 Hz, 1H), 3.36 (t, J = 6.7 Hz, 2H), 2.74 (t, J = 7.6 Hz, 2H), 2.17 (s, 3H), 1.91 (quint, J = 6.9 Hz, 2H), 1.54 (d, J = 7.0 Hz, 3H). ^{13}C NMR (75 MHz, CD_3OD, di-trifluoroacetate) δ (ppm) 179.76, 170.37, 156.02, 143.45, 132.68, 129.70, 128.58, 127.48, 118.35, 54.90, 41.74, 29.71, 23.71, 21.84, 11.53. HRMS (ESI-MS): m/z [M + H$^+$] calculated for $C_{17}H_{25}N_6S_2^+$: 377.1577, found 377.1578; $C_{17}H_{24}N_6S_2$ x 2 TFA (604.59).

4.2.17. 1-(Amino((3-(2-aminothiazol-4-yl)phenyl)amino) methylene)-3-(1-propyl)urea (179)

130 was prepared from **11** (0.06 g, 0.29 mmol), **48** (0.08 g, 0.29 mmol), $HgCl_2$ (0.16 g, 0.58 mmol) and TEA (0.12 mL, 0.87 mmol) in DCM (25 mL) conforming to the general procedure for the guanidinylation reaction. Subsequently, **179** was prepared from the Boc-protected intermediate **130** in DCM (4.0 mL) and TFA (1.0 mL) according to the general procedure (method A) and obtained as a colorless foamlike solid (40 mg, 25%): RP-HPLC: 99%, (t_R = 13.87, k = 3.78). ^{1}H NMR (600 MHz, DMSO-d_6, di-trifluoroacetate): δ (ppm) 10.74 (s, 1H), 10.15 (s, 1H), 8.97 (br s, 1H), 8.62 (br s, 1H), 7.80–7.78 (m, 1H), 7.73–7.72 (m, 1H), 7.60 (t, 1H, J = 5.56 Hz), 7.49 (t, J = 7.74 Hz, 1H), 7.24–7.23 (m, 1H), 7.15 (s, 1H), 3.10–3.06 (m, 2H), 1.49–1.43 (m, 2H), 0.86 (t, J = 7.50 Hz, 3H). ^{13}C NMR (150 MHz, DMSO-d_6, di-trifluoroacetate): δ (ppm) 168.70, 153.60, 153.50, 147.00, 135.50, 134.00, 130.10, 124.84, 124.81, 123.00, 103.00, 41.00, 22.20, 11.20. HRMS (ESI-MS): m/z [M + H$^+$] calculated for $C_{14}H_{19}N_6OS^+$: 319.1336, found 319.1346; $C_{14}H_{18}N_6OS$ x 2 TFA (546.45).

4.2.18. 1-(Amino((2-amino-4,5,6,7-tetrahydrobenzo[d]thiazol-6-yl) amino)methylene)-3-(1-hexyl)urea (185)

136 was prepared from **12** (0.07 g, 0.44 mmol), **50** (0.14 g, 0.44 mmol), $HgCl_2$ (0.24 g, 0.88 mmol) and TEA (0.18 mL, 1.32 mmol) in DCM (25 mL) conforming to the general procedure for the guanidinylation reaction. Subsequently, **185** was prepared from the Boc-protected intermediate **136** in DCM (4.0 mL) and TFA (1.0 mL) according to the general procedure (method A) and obtained as a colorless foamlike solid (46 mg, 18%): RP-HPLC: 95%, (t_R = 17.10, k = 4.90). ^{1}H NMR (600 MHz, DMSO-d_6, di-trifluoroacetate): δ (ppm) 10.17 (s, 1H), 9.07 (s,1H), 8.67 (br s, 4H), 7.50 (s, 1H), 4.05–4.04 (m, 1H), 3.09–3.06 (m, 2H), 2.89–2.86 (m, 1H), 2.60–2.51 (m, 3H), 1.97–1.83 (m, 2H), 1.42–1.39 (m, 2H), 1.29–1.24 (m, 6H), 0.86–0.84 (m, 3H). ^{13}C NMR (150 MHz, DMSO-d_6, di-trifluoroacetate): δ (ppm) 168.90, 154.20, 153.70, 136.50, 112.00, 46.90, 39.49, 31.30, 29.30, 28.40, 26.80, 26.30, 22.50, 21.70, 14.30. HRMS (ESI-MS): m/z [M + H$^+$] calculated for $C_{15}H_{27}N_6OS^+$: 339.1962, found 339.1962; $C_{15}H_{26}N_6OS$ x 2 TFA (566.52).

4.3. Biological assays: experimental protocols

Cell culture. Cells were cultured in 75 cm^2 flasks (Sarstedt, Nümbrecht, Germany) in a humidified atmosphere (95% air, 5% CO_2) at 37 °C. HEK293T-β-Arr2-hH_2R cells [43–45], HEK293T ElucN-βarr2 hD_{2long}R-ELucC cells [54] and HEK293T ElucN-βarr2 hD_3R-ELucC cells [54] were cultured as described previously and regularly monitored for mycoplasma infection using the Venor GeM Mycoplasma Detection Kit (Minerva Biolabs, Berlin, Germany).

Radioligand binding assays. *Histamine $H_{1\text{-}4}$ receptors.* Radioligand competition binding experiments using membranes of Sf9 insect cells co-expressing hH_1R and RGS4, expressing hH_2R-$G_{s\alpha S}$, co-expressing hH_3R, $G\alpha_{i2}$ and $G\beta_1\gamma_2$ or co-expressing hH_4R, $G\alpha_{i2}$ and $G\beta_1\gamma_2$ were performed according to published protocols [14,39]. The following radioligands were used: [^{3}H]mepyramine (hH_1R, specific activity: 20 Ci/mmol, Hartmann Analytics, Braunschweig, Germany or specific activity: 75–87 Ci/mmol, Novandi Chemistry AB, Södertälje, Sweden), [^{3}H]UR-DE257 [38] (hH_2R, specific activity: 63.0 Ci/mmol, was synthesized in our laboratories), [^{3}H]N^α-methylhistamine (specific activity: 85.3 Ci/mmol, Hartmann Analytics) or [^{3}H]UR-PI294 [40] (hH_3R, specific activity: 41.8 Ci/mmol, was synthesized in our laboratories) and [^{3}H]histamine (hH_4R, specific activity: 25 Ci/mmol Hartmann Analytics). Modifications were made as follows: the washing steps were performed with PBS (8 g NaCl, 0.2 g KCl, 1.0 g Na_2HPO_4 x 2H_2O, 0.15 g NaH_2PO_4 x H_2O, 0.1 g KH_2PO_4 in 1 L Millipore H_2O; pH 7.4; 4 °C) instead of binding buffer.

Dopamine $D_{2long,\ 3}$ receptors. Radioligand competition binding experiments using homogenates of HEK293T-CRE-Luc cells expressing hD_{2long}R or hD_3R were performed as described in detail by Forster et al. [54] [^{3}H]*N*-methylspipirone (specific activity: 77 Ci/mmol) was from Novandi Chemistry AB.

[^{35}S]GTPγS binding assay. The [^{35}S]GTPγS binding assay was performed using membranes of Sf9 insect cells expressing the hH_2R-$G_{s\alpha S}$ fusion protein as described in detail by Kagermeier et al. [14] [^{35}S]GTPγS was from PerkinElmer Life Science (Boston, USA) or Hartmann Analytics.

β-Arrestin recruitment assay. The β-arrestin recruitment assays using HEK293T-β-Arr2-hH_2R cells [43,45], HEK293T ElucN-βarr2 hD_{2long}R-ELucC cells [54] or HEK293T ElucN-βarr2 hD_3R-ELucC cells [54] were performed as described previously.

Histamine H_2 receptor assay on the isolated guinea pig right atrium (spontaneously beating). This functional assay was performed as previously described in detail [39].

Data processing. Compound purities were calculated as the

percentage peak area of the analyzed compound by UV detection at 220 nm. Retention factors (k) were calculated from retention times (t_R) according to $k = (t_R - t_0)/t_0$, t_0 = dead time. Data from radioligand binding assays ($H_{1-4}R$ [39]; $D_{2long,\ 3}R$ [54]), [^{35}S]GTPγS binding assay [39,43], β-arrestin 2 recruitment assays (hH_2R [43,45]; $D_{2long,\ 3}R$ [54]), and from H_2R assay on isolated guinea pig right atrium [39] were processed as reported previously.

Nomenclature. Due to their importance as lead compounds (structurally or pharmacologically), the following compounds receive a special compound code: **139** = UR-KAT523, **140** = UR-CH20, **143** = UR-CH22, **145** = UR-Po563, **157** = UR-MB-69, **163** = UR-SB291, **170** = UR-SB257, **172** = UR-KAT527.

Author contributions

S.B., M.B., K.T., C.H. and S.P. performed the synthesis and the analytical characterization of chemical compounds. M.B. performed the determination of pK_a values. C.H. performed the investigation of the chemical stability. S.P. performed the determination of the enantiomeric purities. S.B., M.B., K.T., C.H. and S.P performed the radioligand competition binding experiments ($hH_{1-4}R$). L.F. performed the radioligand competition binding experiments ($hD_{2long/3}R$). S.B. performed the [^{35}S]GTPγS binding experiments. S.B. and K.T. performed the β-arrestin2 recruitment assays at the hH_2R. L.F. and K.T. performed the β-arrestin2 recruitment assays at the $hD_{2long}R$ and hD_3R. M.B. and S.P performed the guinea pig right atrium experiments. A.B. initiated the project. A.B., G.B. and S.P. supervised the research. S.B., M.B., K.T. and S.P. wrote the manuscript. All authors have given their approval for the final version of the manuscript. S.B., M.B. and K.T. contributed equally.

Funding sources

This work was supported by the Graduate Training Program (Graduiertenkolleg) GRK1910 “Medicinal chemistry of selective ligands” of the Deutsche Forschungsgemeinschaft (DFG) (S.B., K.T. A.B., and G.B.).

Declaration of competing interest

The authors declare that they have no known competing financial interests or personal relationships that could have appeared to influence the work reported in this paper.

Acknowledgment

The authors thank Maria Beer-Krön, Sieglinde Dechant, Christine Braun and Kerstin Röhrl for excellent technical assistance. We thank Dr. Anja Kraus for providing the branched carboxylic acids **40**–**47** and Dr. Tobias Birnkammer for providing the compounds UR-BIT22, UR-BIT23 and UR-BIT29. We thank Dr. Harald Hübner (Department of Chemistry and Pharmacy, Friedrich-Alexander-University Erlangen-Nürnberg) for providing the cDNAs of the $hD_{2long}R$ and the hD_3R and his insightful advice on binding assays at dopamine $D_{2long/3}$ receptors. We also thank Dr. Johannes Felixberger for providing the HEK293T-β-Arr2-hH_2R cells. We thank Josef Kiermaier and Wolfgang Söllner for mass spectrometry analysis. We thank Fritz Kastner for NMR measurements and Michael A. Walters for proof reading.

Appendix A. Supplementary data

Supplementary data to this article can be found online at https://doi.org/10.1016/j.ejmech.2021.113190.

Abbreviations

α	intrinsic activity
β-Arr2 or βarr2	β-arrestin2 gene and protein
δ	chemical shift in ppm
APCI	atmospheric pressure chemical ionization
Ar	argon
AU	absorption units
Boc	tert-butoxycarbonyl
cat	catalyst
$CDCl_3$	deuterated chloroform
cf.	confer/conferatur
CRE-Luc	cAMP-response element driven transcriptional luciferase reporter
CD_3OD	deuterated methanol
CNS	central nervous system
cmpd	compound
DAD	diode array detector
DCM	dichloromethane
DEPT	distortionless enhancement by polarization transfer
DIPEA	diisopropylethylamine or Hün
DMF	dimethylformamide
DMSO	dimethyl sulfoxide
DMSO-d_6	deuterated DMSO
D_xR	dopamine receptor subtype x
e.g.	exempli gratia
EI	electron ionization
Eluc	Emerald luciferase
ElucC	C-terminal Eluc fragment
ElucN	N-terminal Eluc fragment
ESI	electrospray ionization
EtOAc	ethyl acetate
equiv	equivalent
EtOH	ethanol
$G\alpha_{i2}$	α-subunit of the G_{i2} protein that mediates inhibition of adenyl cyclase
$G\beta_1\gamma_2$	G protein β_1-and γ_2-subunit
gp	guinea pig
$G_{s\alpha S}$	α-subunit (short splice variant) of the G_s protein that mediates stimulation of adenylyl cyclase
GPCR	G protein coupled receptor
GTPγS	guanosine 5′-O-[gamma-thio]phosphate
h	human
HR	histamine receptor
HEK293T	human embryonic kidney 293T cells
HPLC	high-performance liquid chromatography
HRMS	high-resolution mass spectrometry
H_xR	histamine receptor subtype x
J	coupling constant (NMR)
k	retention (or capacity) factor (HPLC)
K_a	acid dissociation constant
K_b	dissociation constant obtained from functional assays
K_d	dissociation constant obtained from a saturation binding experiment
K_i	dissociation constant obtained from a competition binding experiment
LC	liquid chromatography
MeCN	acetonitrile
MeOH	methanol
MS	mass spectrometry
m/z	mass-to-charge ratio
NMR	nuclear magnetic resonance
PE	petroleum ether
pEC_{50}	negative logarithm of the half-maximum activity concentration in M

pH	potential or power of hydrogen
pK_a	negative logarithm of the K_a
pK_b	negative logarithm of the K_b in M
pK_i	negative logarithm of the K_i in M
ppm	parts per million
R	residue
R_f	retention factor (in TLC) RGS4 regulator of G protein signaling proteins 4
RP-HPLC	reversed-phase HPLC
rt	room temperature
Q-TOF	quadrupole time of flight
SEM	standard error of the mean
Sf9	*Spodoptera frugiperda* insect cell line
SM	supplementary material
t_0	dead time
TEA	triethylamine
TLC	thin layer chromatography
TFA	trifluoroacetic acid
t_R	retention time
Trt	trityl
UHD	ultra high definition
UV	ultraviolet

References

[1] B.K. Kobilka, G protein coupled receptor structure and activation, Biochim. Biophys. Acta Biomembr. 1768 (2007) 794–807.

[2] D.M. Rosenbaum, S.G.F. Rasmussen, B.K. Kobilka, The structure and function of G-protein-coupled receptors, Nature 459 (2009) 356–363.

[3] S.J. Hill, C.R. Ganellin, H. Timmerman, J.C. Schwartz, N.P. Shankley, J.M. Young, W. Schunack, R. Levi, H.L. Haas, International union of pharmacology. XIII. Classification of histamine receptors, Pharmacol. Rev. 49 (1997) 253–278.

[4] P. Panula, P.L. Chazot, M. Cowart, R. Gutzmer, R. Leurs, W.L. Liu, H. Stark, R.L. Thurmond, H.L. Haas, International union of basic and clinical pharmacology. XCVIII. Histamine receptors, Pharmacol. Rev. 67 (2015) 601–655.

[5] L.B. Hough, Genomics meets histamine receptors: new subtypes, new receptors, Mol. Pharmacol. 59 (2001) 415–419.

[6] S.M. Foord, T.I. Bonner, R.R. Neubig, E.M. Rosser, J.P. Pin, A.P. Davenport, M. Spedding, A.J. Harmar, International union of pharmacology. XLVI. G protein-coupled receptor list, Pharmacol. Rev. 57 (2005) 279–288.

[7] J.W. Black, W.A.M. Duncan, G.J. Durant, C.R. Ganellin, M.E. Parsons, Definition and antagonism of histamine H_2-receptors, Nature 236 (1972) 385–390.

[8] E. Traiffort, H. Pollard, J. Moreau, M. Ruat, J.C. Schwartz, M.I. Martinez-Mir, J.M. Palacios, Pharmacological characterization and autoradiographic localization of histamine H_2 receptors in human brain identified with [^{125}I]iodoaminopotentidine, J. Neurochem. 59 (1992) 290–299.

[9] S. Dove, S. Elz, R. Seifert, A. Buschauer, Structure-activity relationships of histamine H_2 receptor ligands, Mini Rev. Med. Chem. 4 (2004) 941–954.

[10] P. Ghorai, A. Kraus, M. Keller, C. Götte, P. Igel, E. Schneider, D. Schnell, G. Bernhardt, S. Dove, M. Zabel, S. Elz, R. Seifert, A. Buschauer, Acylguanidines as bioisosteres of guanidines: N^G-acylated imidazolylpropylguanidines, a new class of histamine H_2 receptor agonists, J. Med. Chem. 51 (2008) 7193–7204.

[11] A. Kraus, P. Ghorai, T. Birnkammer, D. Schnell, S. Elz, R. Seifert, S. Dove, G. Bernhardt, A. Buschauer, N^G-Acylated aminothiazolylpropylguanidines as potent and selective histamine H_2 receptor agonists, ChemMedChem 4 (2009) 232–240.

[12] A. Kraus, Highly Potent, Selective Acylguanidine-type Histamine H_2 Receptor Agonists: Synthesis and Structure-Activity Relationships, PhD Thesis, University of Regensburg, 2007.

[13] T. Birnkammer, A. Spickenreither, I. Brunskole, M. Lopuch, N. Kagermeier, G. Bernhardt, S. Dove, R. Seifert, S. Elz, A. Buschauer, The bivalent ligand approach leads to highly potent and selective acylguanidine-type histamine H_2 receptor agonists, J. Med. Chem. 55 (2012) 1147–1160.

[14] N. Kagermeier, K. Werner, M. Keller, P. Baumeister, G. Bernhardt, R. Seifert, A. Buschauer, Dimeric carbamoylguanidine-type histamine H_2 receptor ligands: a new class of potent and selective agonists, Bioorg. Med. Chem. 23 (2015) 3957–3969.

[15] C.A. Lipinski, F. Lombardo, B.W. Dominy, P.J. Feeney, Experimental and computational approaches to estimate solubility and permeability in drug discovery and development settings, Adv. Drug Deliv. Rev. 23 (1997) 3–25.

[16] A.K. Ghose, V.N. Viswanadhan, J.J. Wendoloski, A knowledge-based approach in designing combinatorial or medicinal chemistry libraries for drug discovery. 1. A qualitative and quantitative characterization of known drug databases, J. Comb. Chem. 1 (1999) 55–68.

[17] M.D. Shultz, Two decades under the influence of the rule of five and the changing properties of approved oral drugs, J. Med. Chem. 62 (2019) 1701–1714.

[18] J.P. Bennett Jr., M.F. Piercey, Pramipexole-a new dopamine agonist for the treatment of Parkinson's disease, J. Neurol. Sci. 163 (1999) 25–31.

[19] A. Morrell, M.S. Placzek, J.D. Steffen, S. Antony, K. Agama, Y. Pommier, M. Cushman, Investigation of the lactam side chain length necessary for optimal indenoisoquinoline topoisomerase I inhibition and cytotoxicity in human cancer cell cultures, J. Med. Chem. 50 (2007) 2040–2048.

[20] M. Johnson, T. Antonio, M.E.A. Reith, A.K. Dutta, Structure–activity relationship study of N^6-(2-(4-(1H-indol-5-yl)piperazin-1-yl)ethyl)-N^6-propyl-4,5,6,7-tetrahydrobenzo[d]thiazole-2,6-diamine analogues: development of highly selective D_3 dopamine receptor agonists along with a highly potent D_2/D_3 agonist and their pharmacological characterization, J. Med. Chem. 55 (2012) 5826–5840.

[21] Z. Li, R.J. Mayer, A.R. Ofial, H. Mayr, From carbodiimides to carbon dioxide: quantification of the electrophilic reactivities of heteroallenes, J. Am. Chem. Soc. 142 (2020) 8383–8402.

[22] D.T. Manallack, The pK_a distribution of drugs: application to drug discovery, Perspect. Med. Chem. 1 (2007) 25–38.

[23] M. Gabryszewski, J. Kulig, B. Lenarcik, Stability and structure of transition metal complexes with azoles in aqueous solutions. Part 24. Comparison of complex forming ability of methylthiazoles and aminothiazoles, Pol. J. Chem. 56 (1982) 55–60.

[24] L. Forlani, A.L. Tocke, E. Del Vecchio, S. Lakhdar, R. Goumont, F. Terrier, Assessing the nitrogen and carbon nucleophilicities of 2-aminothiazoles through coupling with superelectrophilic 4,6-dinitrobenzofuroxan, J. Org. Chem. 71 (2006) 5527–5537.

[25] A.S. Al-Attas, M.M. Habeeb, D.S. Al-Raimi, Spectrophotometric determination of some amino heterocyclic donors through charge transfer complex formation with chloranilic acid in acetonitrile, J. Mol. Liq. 148 (2009) 58–66.

[26] M. Nagano, T. Matsui, J. Tobitsuka, K. Oyamada, Studies on organic sulfur compounds. IX. The reaction of ethoxycarbonyl isothiocyanate with 4, 5-substituted 2-aminothiazoles, Chem. Pharm. Bull. 20 (1972) 2626–2633.

[27] A. Daina, O. Michielin, V. Zoete, SwissADME: a free web tool to evaluate pharmacokinetics, drug-likeness and medicinal chemistry friendliness of small molecules, Sci. Rep. 7 (2017), 42717-42717.

[28] Y.C. Martin, A bioavailability score, J. Med. Chem. 48 (2005) 3164–3170.

[29] T. Okura, R. Ito, N. Ishiguro, I. Tamai, Y. Deguchi, Blood-brain barrier transport of pramipexole, a dopamine D_2 agonist, Life Sci. 80 (2007) 1564–1571.

[30] H. Pajouhesh, G.R. Lenz, Medicinal chemical properties of successful central nervous system drugs, NeuroRx 2 (2005) 541–553.

[31] A. Daina, O. Michielin, V. Zoete, iLOGP: a simple, robust, and efficient description of n-octanol/water partition coefficient for drug design using the GB/SA approach, J. Chem. Inf. Model. 54 (2014) 3284–3301.

[32] T. Cheng, Y. Zhao, X. Li, F. Lin, Y. Xu, X. Zhang, Y. Li, R. Wang, L. Lai, Computation of octanol-water partition coefficients by guiding an additive model with knowledge, J. Chem. Inf. Model. 47 (2007) 2140–2148.

[33] S.A. Wildman, G.M. Crippen, Prediction of physicochemical parameters by atomic contributions, J. Chem. Inf. Comput. Sci. 39 (1999) 868–873.

[34] I. Moriguchi, H. Shuichi, Q. Liu, I. Nakagome, Y. Matsushita, Simple method of calculating octanol/water partition coefficient, Chem. Pharm. Bull. 40 (1992) 127–130.

[35] I. Moriguchi, H. Shuichi, I. Nakagome, H. Hirano, Comparison of reliability of log P values for drugs calculated by several methods, Chem. Pharm. Bull. 42 (1994) 976–978.

[36] J.S. Delaney, ESOL: estimating aqueous solubility directly from molecular structure, J. Chem. Inf. Comput. Sci. 44 (2004) 1000–1005.

[37] S.A.A. Anand, C. Loganathan, N.S. Thomas, K. Saravanan, A.T. Alphonsa, S. Kabilan, Synthesis, structure prediction, pharmacokinetic properties, molecular docking and antitumor activities of some novel thiazinone derivatives, New J. Chem. 39 (2015) 7120–7129.

[38] P. Baumeister, D. Erdmann, S. Biselli, N. Kagermeier, S. Elz, G. Bernhardt, A. Buschauer, [^{3}H]UR-DE257: development of a tritium-labeled squaramide-type selective histamine H_2 receptor antagonist, ChemMedChem 10 (2015) 83–93.

[39] S. Pockes, D. Wifling, M. Keller, A. Buschauer, S. Elz, Highly potent, stable, and selective dimeric hetarylpropylguanidine-type histamine H_2 receptor agonists, ACS Omega 3 (2018) 2865–2882.

[40] P. Igel, D. Schnell, G. Bernhardt, R. Seifert, A. Buschauer, Tritium-labeled N^1-[3-(1*H*-imidazol-4-yl)propyl]-N^2-propionylguanidine ([^{3}H]UR-PI294), a high-affinity histamine H_3 and H_4 receptor radioligand, ChemMedChem 4 (2009) 225–231.

[41] S. Elz, K. Kramer, H.H. Pertz, H. Detert, A.M. ter Laak, R. Kühne, W. Schunack, Histaprodifens: synthesis, pharmacological in vitro evaluation, and molecular modeling of a new class of highly active and selective histamine H_1-receptor agonists, J. Med. Chem. 43 (2000) 1071–1084.

[42] M.T. Kelley, T. Bürckstürmmer, K. Wenzel-Seifert, S. Dove, A. Buschauer, R. Seifert, Distinct interaction of human and Guinea pig histamine H_2-receptor with guanidine-type agonists, Mol. Pharmacol. 60 (2001) 1210–1225.

[43] S. Biselli, I. Alencastre, K. Tropmann, D. Erdmann, M. Chen, T. Littmann, A.F. Maia, M. Gomez-Lazaro, M. Tanaka, T. Ozawa, M. Keller, M. Lamghari, A. Buschauer, G. Bernhardt, Fluorescent H_2 receptor squaramide-type antagonists: synthesis, characterization and applications, ACS Med. Chem. Lett. 11 (2020) 1521–1528.

[44] J. Felixberger, Luciferase Complementation for the Determination of Arrestin Recruitment: Investigation of Histamine and NPY Receptors, Ph.D. Thesis, University of Regensburg, 2014.

[45] L. Grätz, K. Tropmann, M. Bresinsky, C. Müller, G. Bernhardt, S. Pockes, NanoBRET binding assay for histamine H_2 receptor ligands using live recombinant HEK293T cells, Sci. Rep. 10 (2020) e13288.
[46] D.C. Hornigold, R. Mistry, P.D. Raymond, J.L. Blank, R.A.J. Challiss, Evidence for cross-talk between M_2 and M_3 muscarinic acetylcholine receptors in the regulation of second messenger and extracellular signal-regulated kinase signalling pathways in Chinese hamster ovary cells, Br. J. Pharmacol. 138 (2003) 1340–1350.
[47] P. Chidiac, S. Nouet, M. Bouvier, Agonist-induced modulation of inverse agonist efficacy at the beta 2-adrenergic receptor, Mol. Pharmacol. 50 (1996) 662–669.
[48] A. Newman-Tancredi, D. Cussac, L. Marini, M.J. Millan, Antibody capture assay reveals bell-shaped concentration-response isotherms for h5-HT_{1A} receptor-mediated $G\alpha_{i3}$ activation: conformational selection by high-efficacy agonists, and relationship to trafficking of receptor signaling, Mol. Pharmacol. 62 (2002) 590–601.
[49] T. Moriguchi, H. Matsuura, Y. Itakura, H. Katsuki, H. Saito, N. Nishiyama, Allixin, a phytoalexin produced by garlic, and its analogues as novel exogenous substances with neurotrophic activity, Life Sci. 61 (1997) 1413–1420.
[50] O. Zegarra-Moran, L. Romio, C. Folli, E. Caci, F. Becq, J.M. Vierfond, Y. Mettey, G. Cabrini, P. Fanen, L.J. Galietta, Correction of G551D-CFTR transport defect in epithelial monolayers by genistein but not by CPX or MPB-07, Br. J. Pharmacol. 137 (2002) 504–512.
[51] K.A. Wreggett, J.W. Wells, Cooperativity manifest in the binding properties of purified cardiac muscarinic receptors, J. Biol. Chem. 270 (1995) 22488–22499.
[52] S.C. Owen, A.K. Doak, A.N. Ganesh, L. Nedyalkova, C.K. McLaughlin, B.K. Shoichet, M.S. Shoichet, Colloidal drug formulations can explain "bell-shaped" concentration-response curves, ACS Chem. Biol. 9 (2014) 777–784.
[53] J. Chen, C. Jiang, B. Levant, X. Li, T. Zhao, B. Wen, R. Luo, D. Sun, S. Wang, Pramipexole derivatives as potent and selective dopamine D_3 receptor agonists with improved human microsomal stability, ChemMedChem 9 (2014) 2653–2660.
[54] L. Forster, L. Grätz, D. Mönnich, G. Bernhardt, S. Pockes, A split luciferase complementation assay for the quantification of β-arrestin2 recruitment to dopamine D_2-like receptors, Int. J. Mol. Sci. 21 (2020) 6103.
[55] S. Pockes, D. Wifling, A. Buschauer, S. Elz, Structure-activity relationship of hetarylpropylguanidines aiming at the development of selective histamine receptor ligands, ChemistryOpen 8 (2019) 285–297.